Alpine Glaciation

Mer de Glace, Mont Blanc Massif, France


Southeast Greenland, 3 July 2012

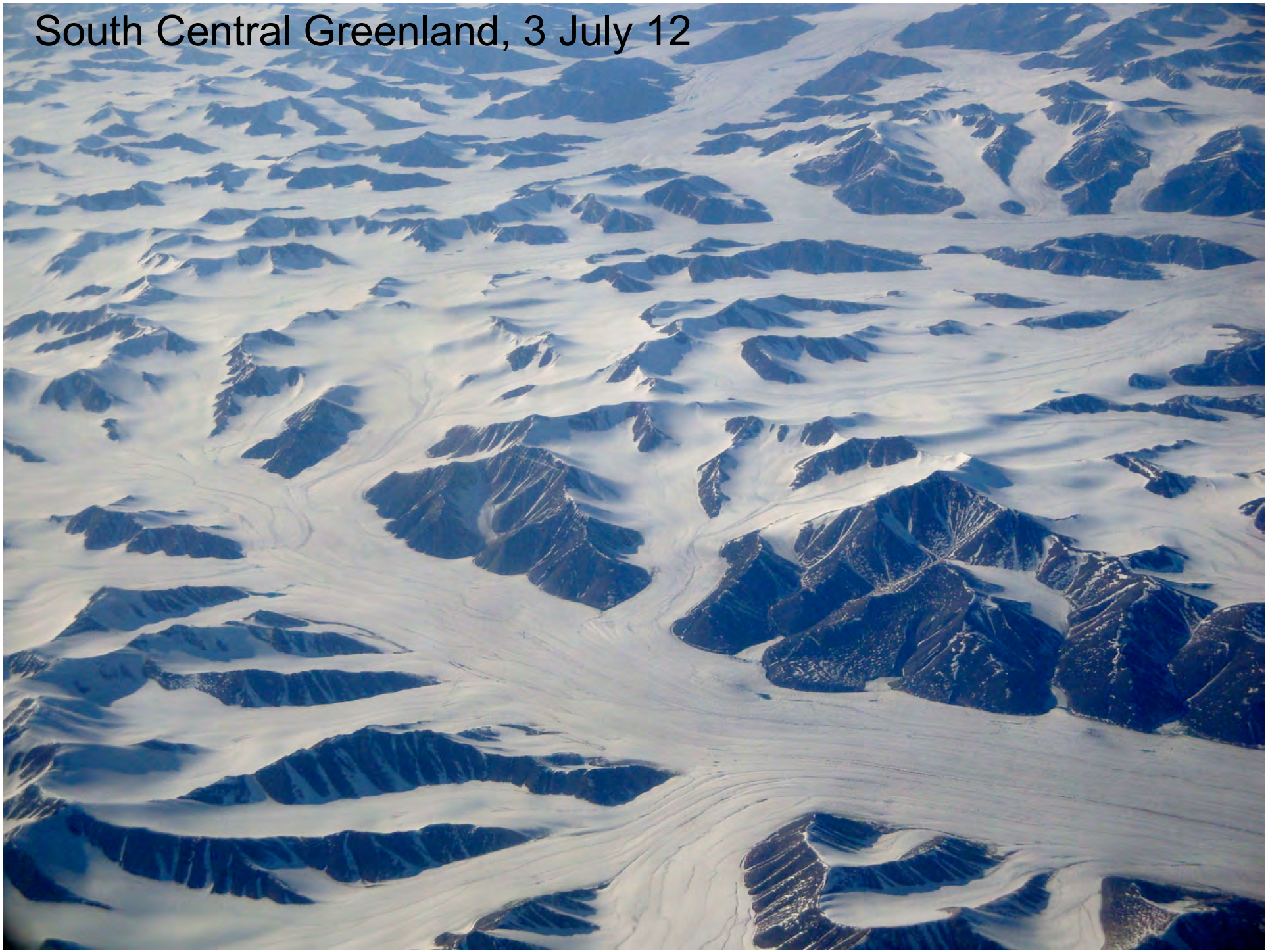
South Central Greenland, 3 July 12

Greenland Ice Sheet:

contours indicate elevation of ice sheet above sea level

Fig. 12.5

Antarctic Ice Sheets

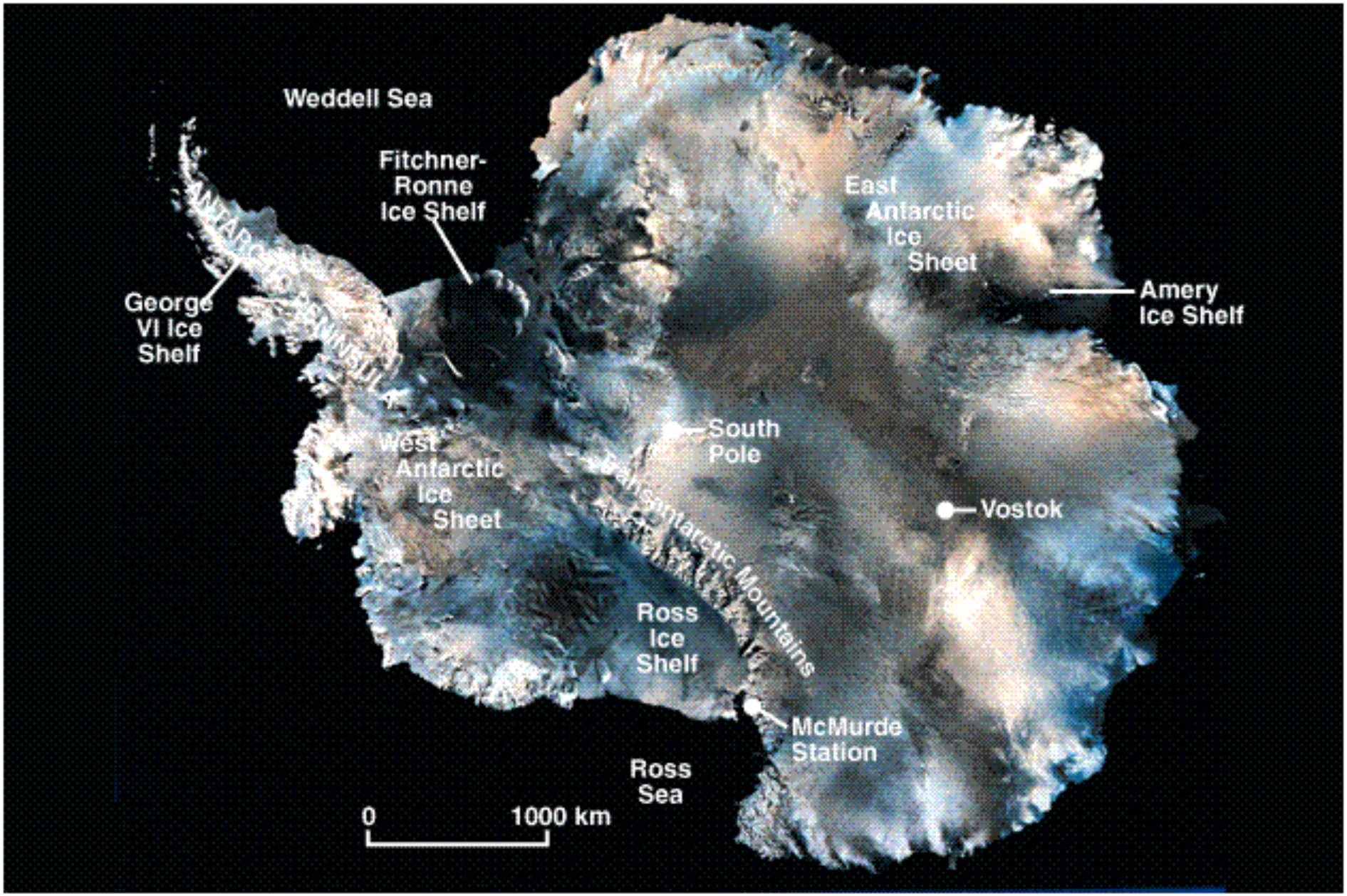

- A large body of moving ice
- Formed on land
- Recrystallization of snow
- Types:
  - Alpine (valley) glaciers
  - Continental glaciers


Rhone Valley, Les Bossons, France

Distribution of alpine glaciation in the Lower 48

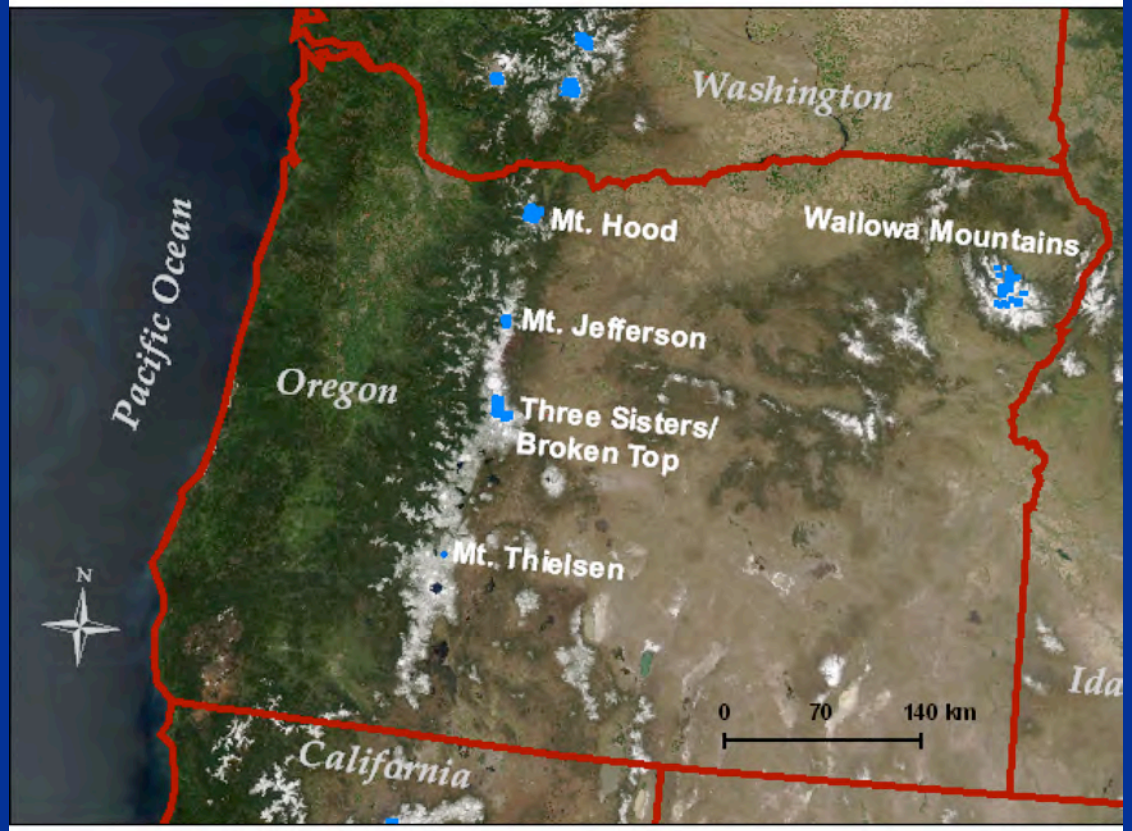

Present Glaciers Oregon

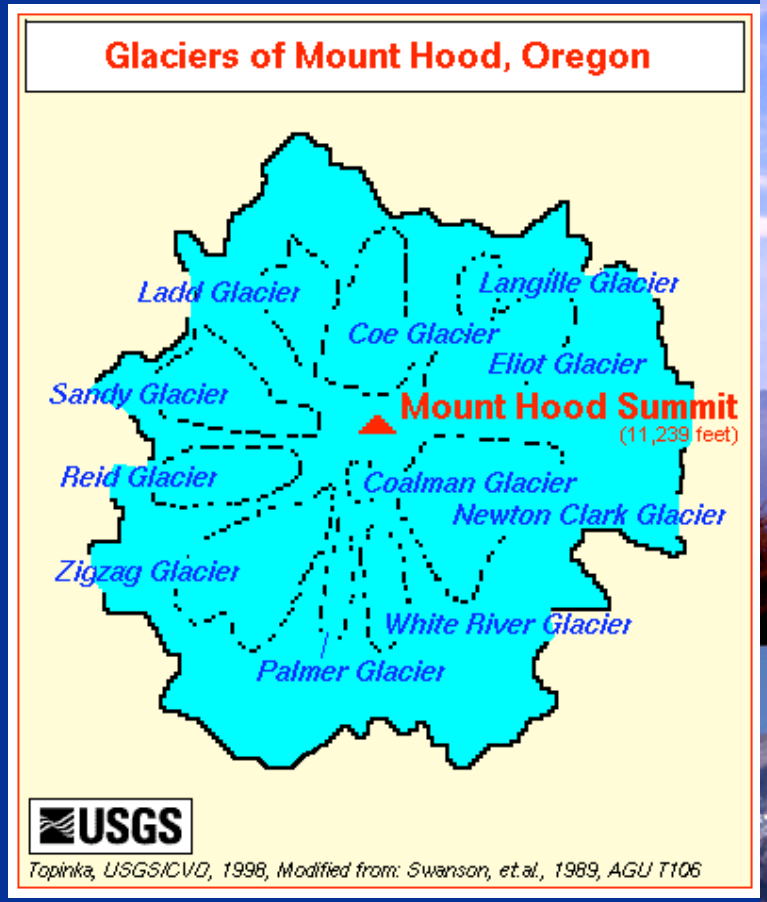
Glaciers of Mount Hood, Oregon
Ladd Glacier
Langille Glacier
Coe Glacier
Eliot Glacier
Sandy Glacier
Mount Hood Summit
(11,239 feet)
Reid Glacier
Coalman Glacier
Newton Clark Glacier
Zigzag Glacier
White River Glacier
Palmer Glacier
USGS
Topinka, USGS/CVO, 1998, Modified from: Swanson, et.al., 1989, AGU T106


Mt Hood North Side

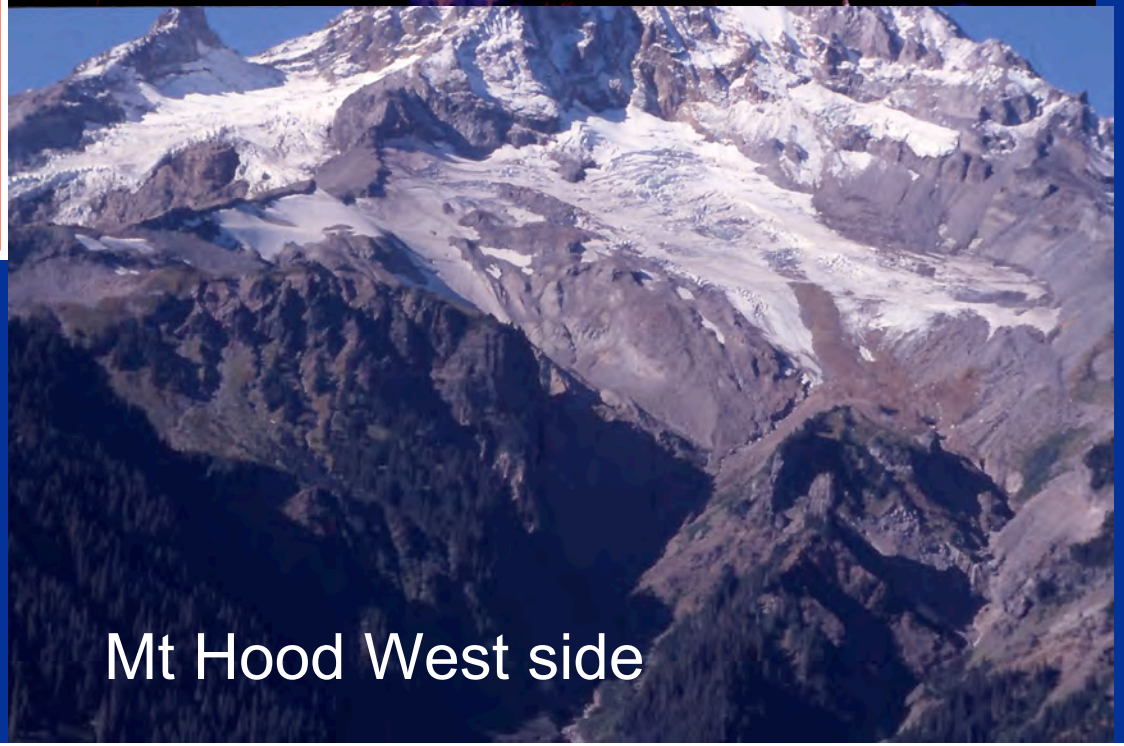
Mt Hood West side

Elliott Glacier 1935

Elliott Glacier 2005

http://glaciers.research.pdx.edu/states/oregon.php#Glacier_Change

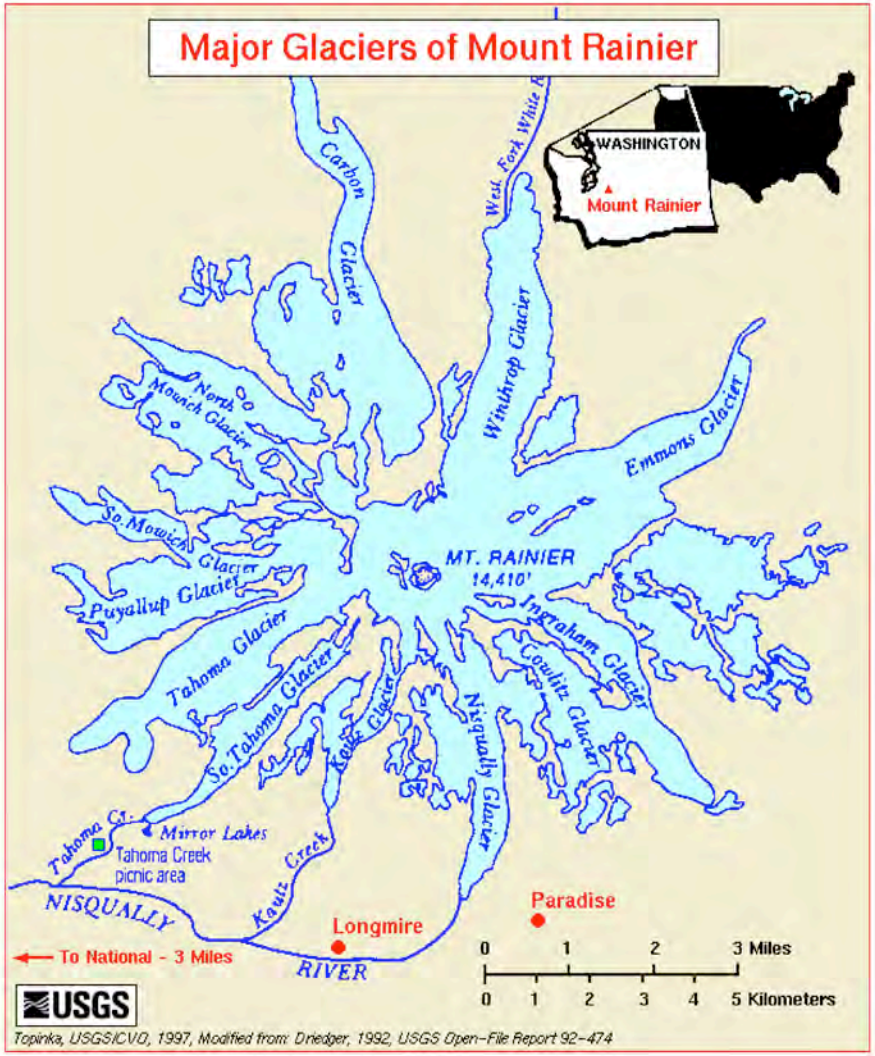

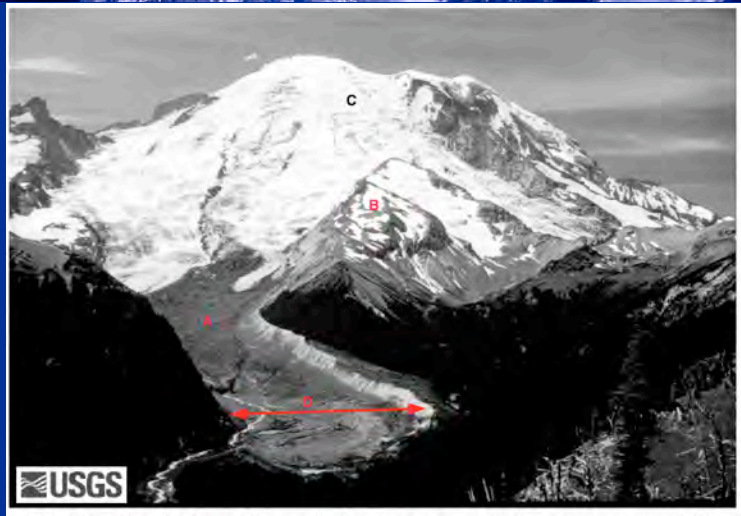

NE flank Mt Rainer, with Osceola Mudflow (A). The mudflow formed 5600 BP when the crater wall (C) collapsed, sending debris across Steamboat Prowl (B) and then down the White River canyon (D)

Courtesy USGS

Mountain Landscape before Glaciation

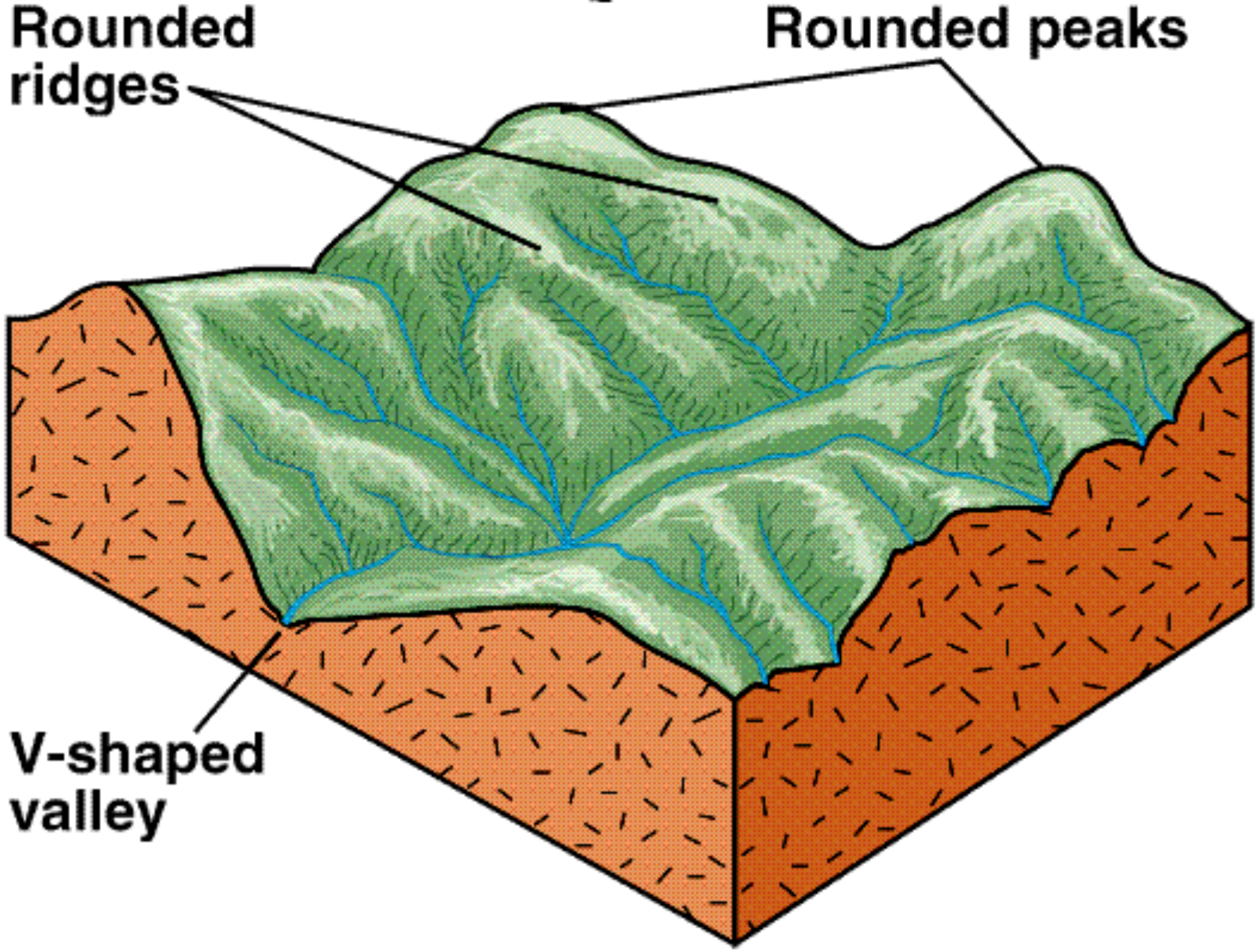

A

Mountain Landscape during Glaciation

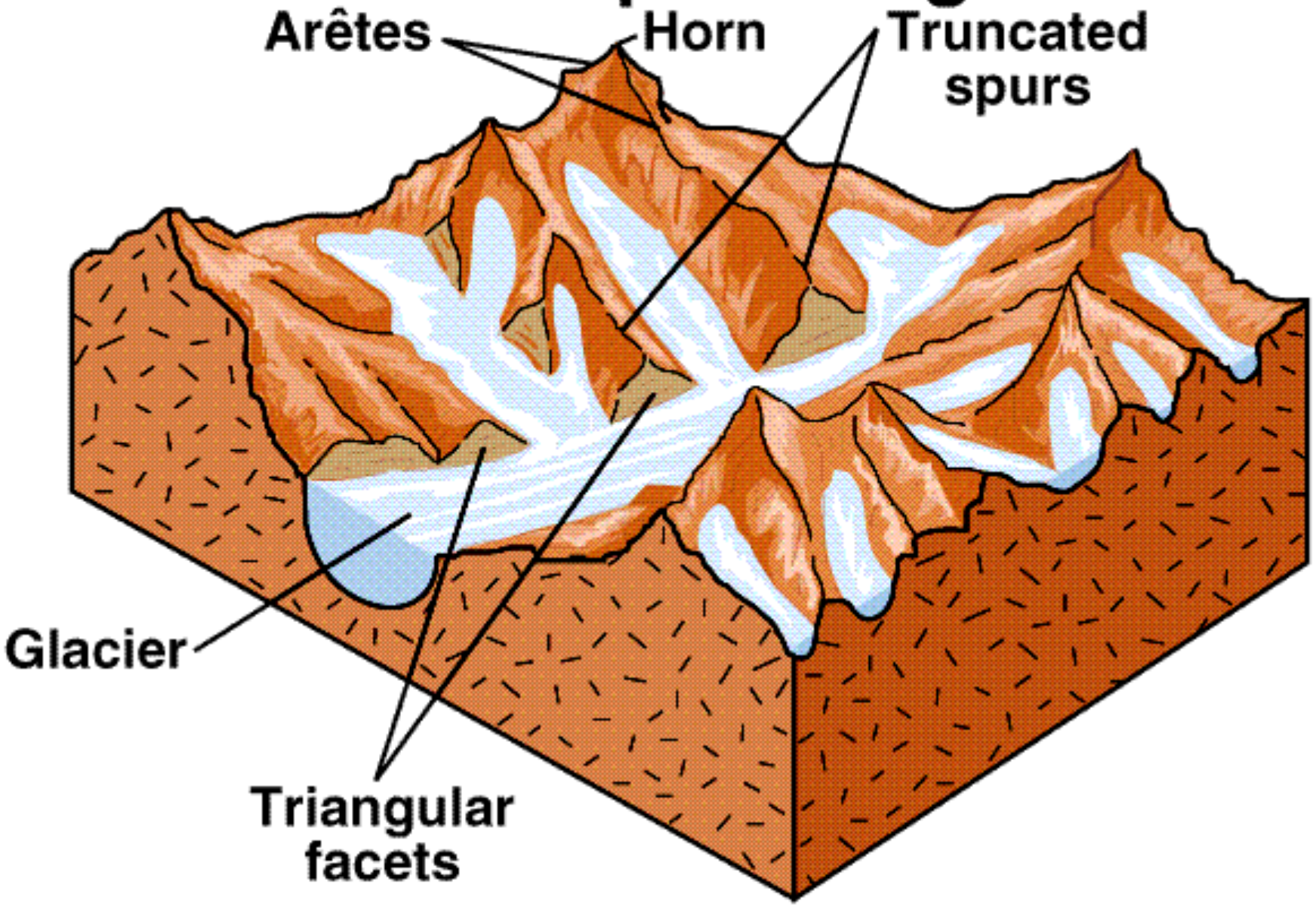

B

Glacier Wastage

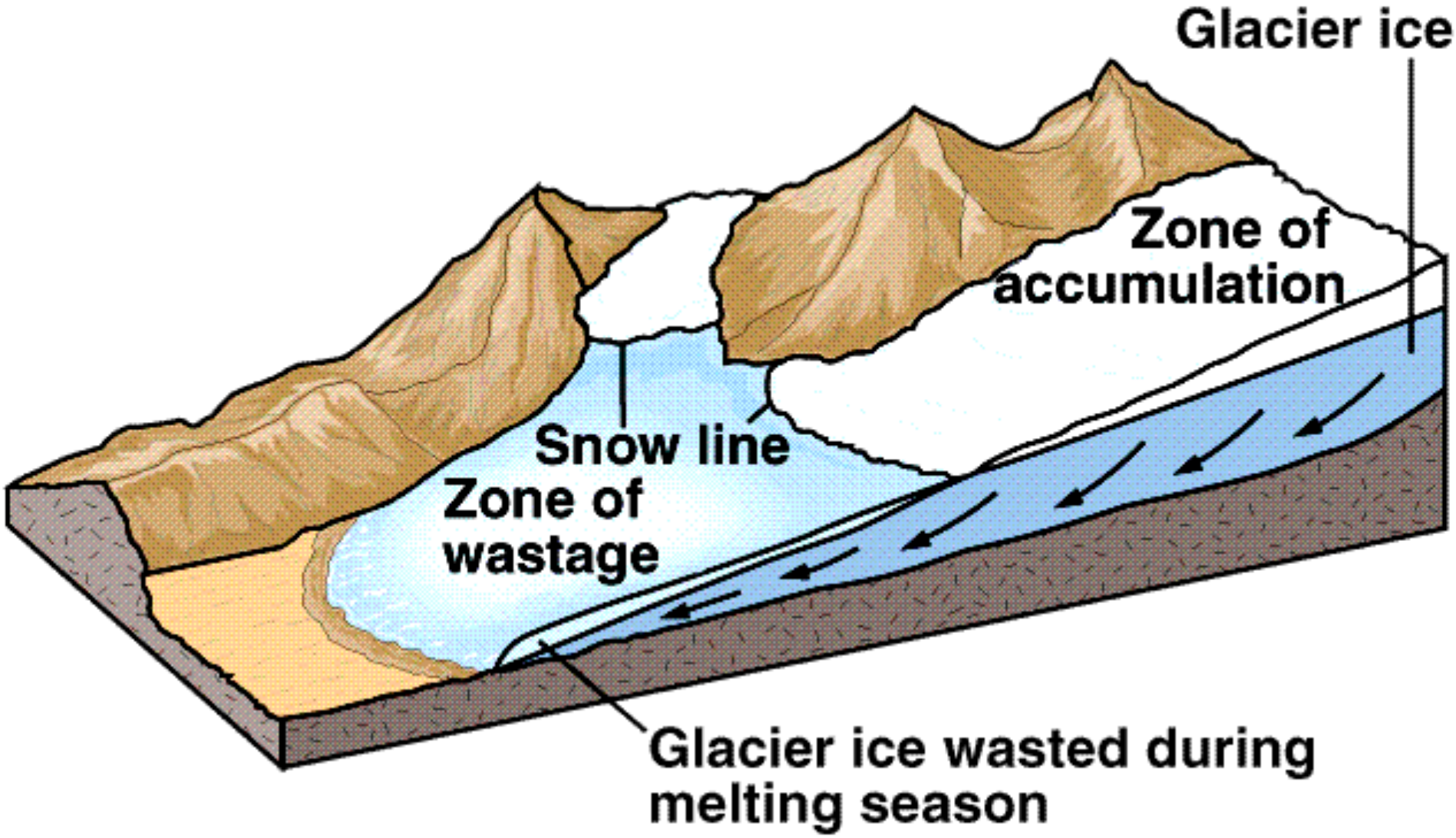

Mountain Landscape after Glaciation

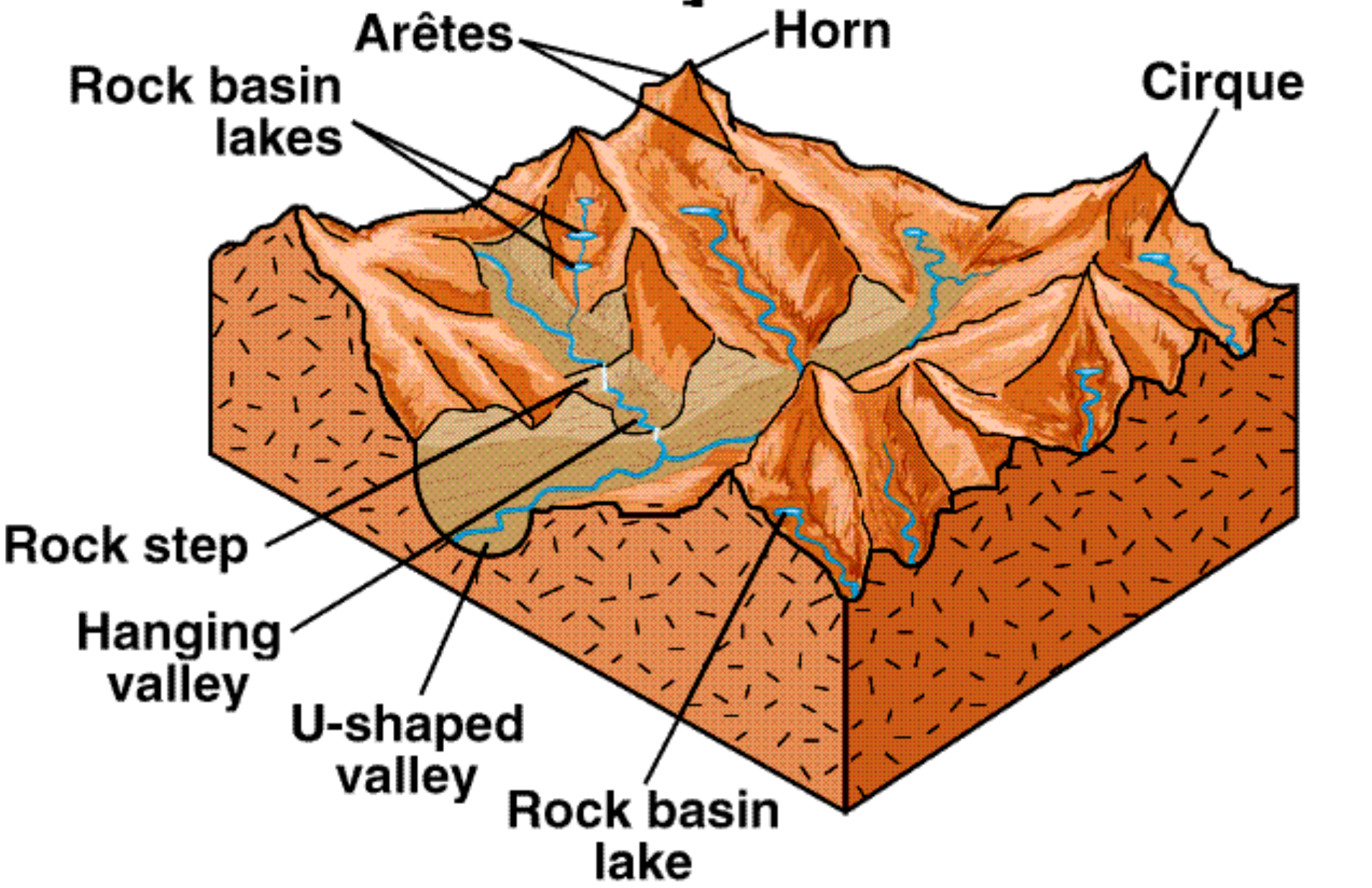

C

Ice Sheet

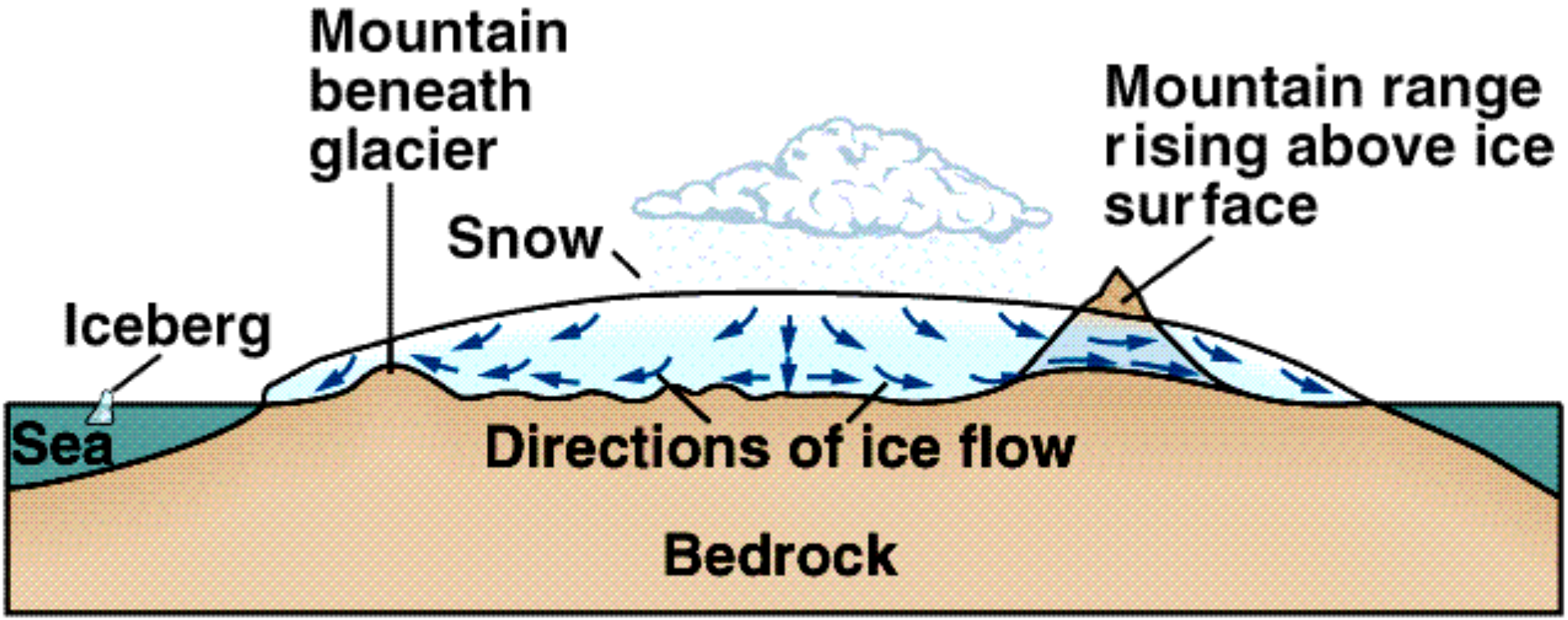

Plucking and Abrasion beneath Glacier

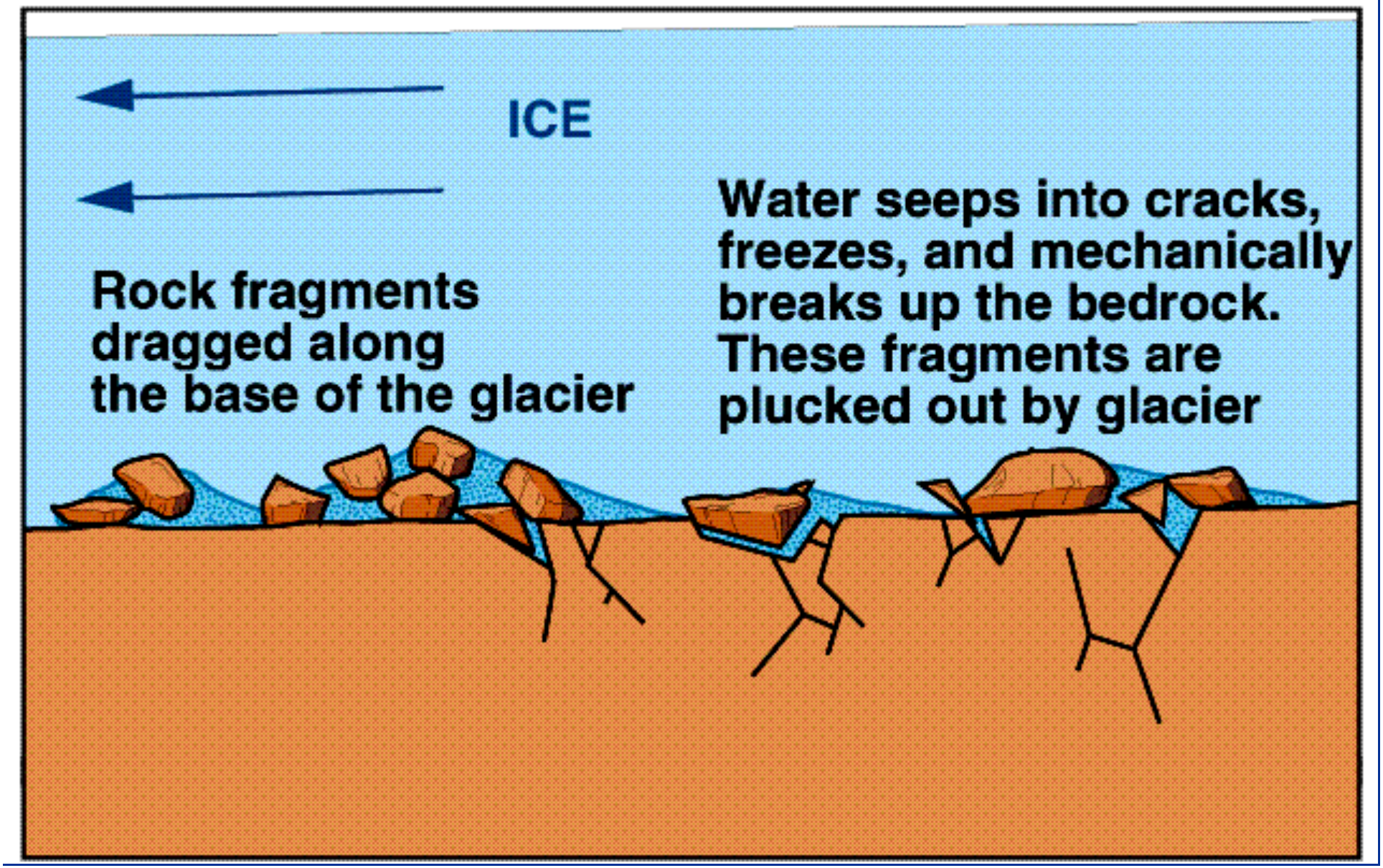

Receding Ice Sheets and Deposition

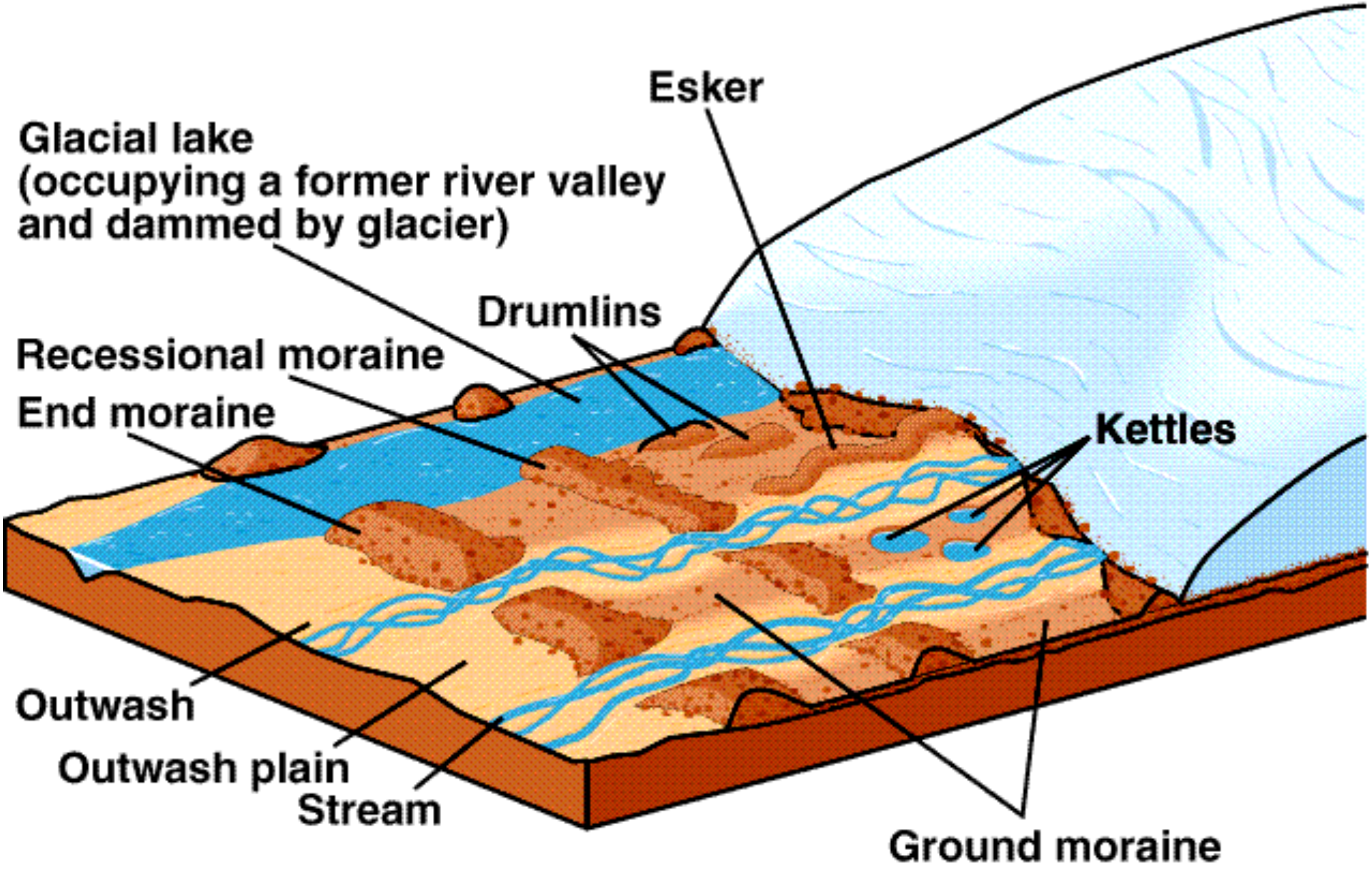

Glacial Striation

Medial and Lateral Moraines

Glacial Erratic, Alberta

A Kettle and Outwash

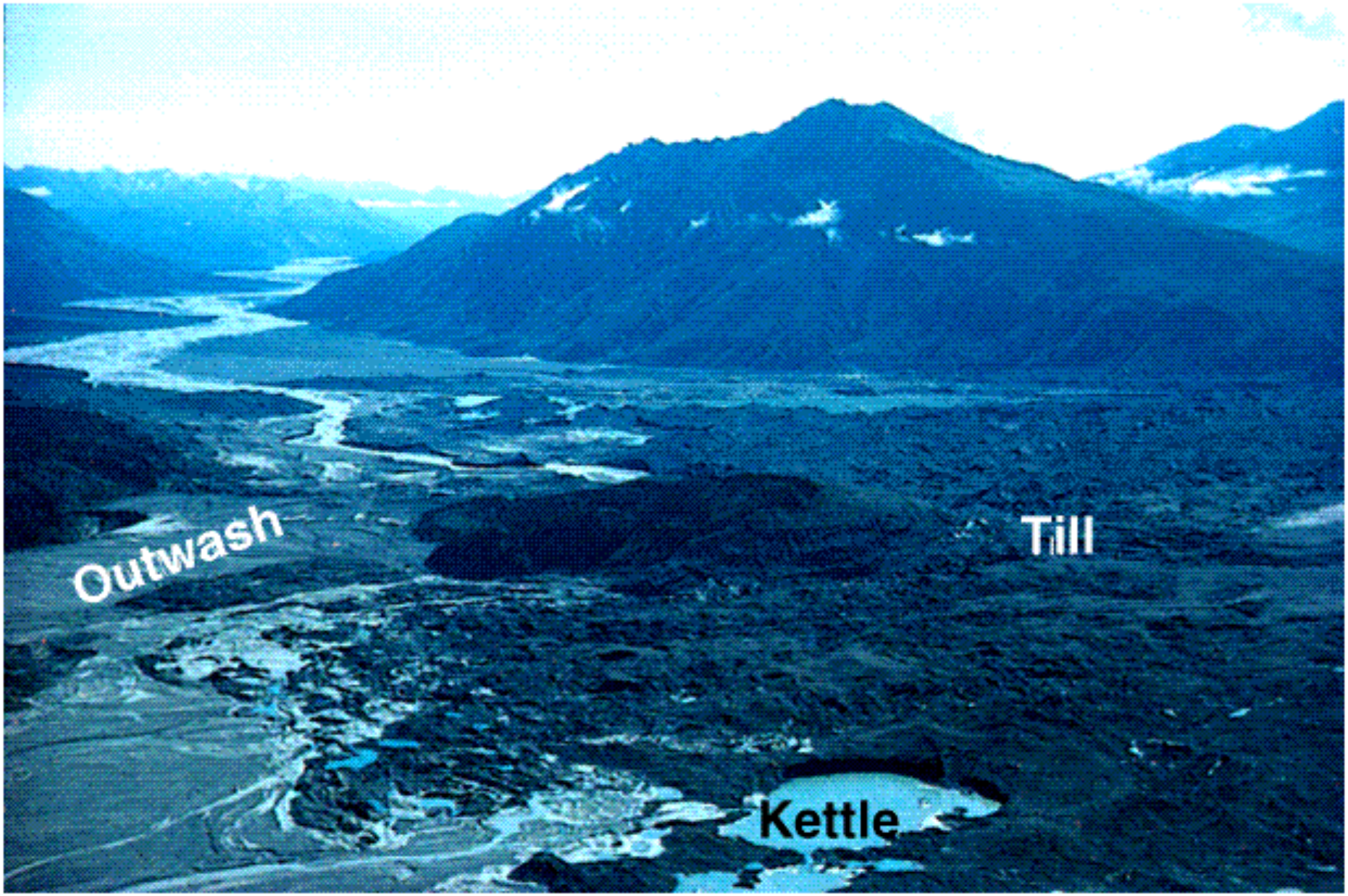

Quaternary Glacial History

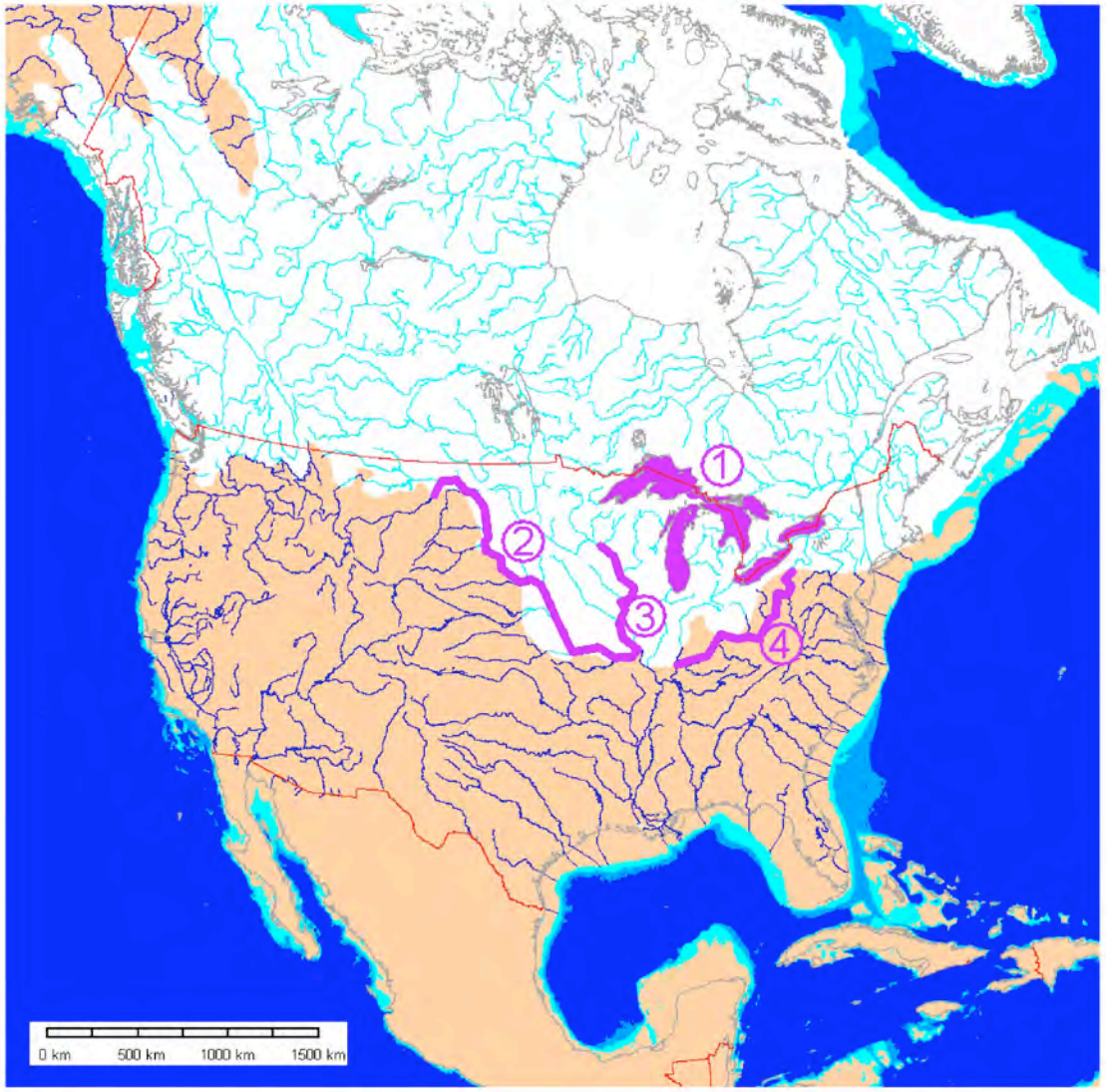

Glacial Maximum North America

Major Effects:

1. Great Lakes
2. Missouri River Drainage
3. Upper Mississippi River Drainage
4. Ohio River Drainage

North American Moraines and Pluvial Lakes

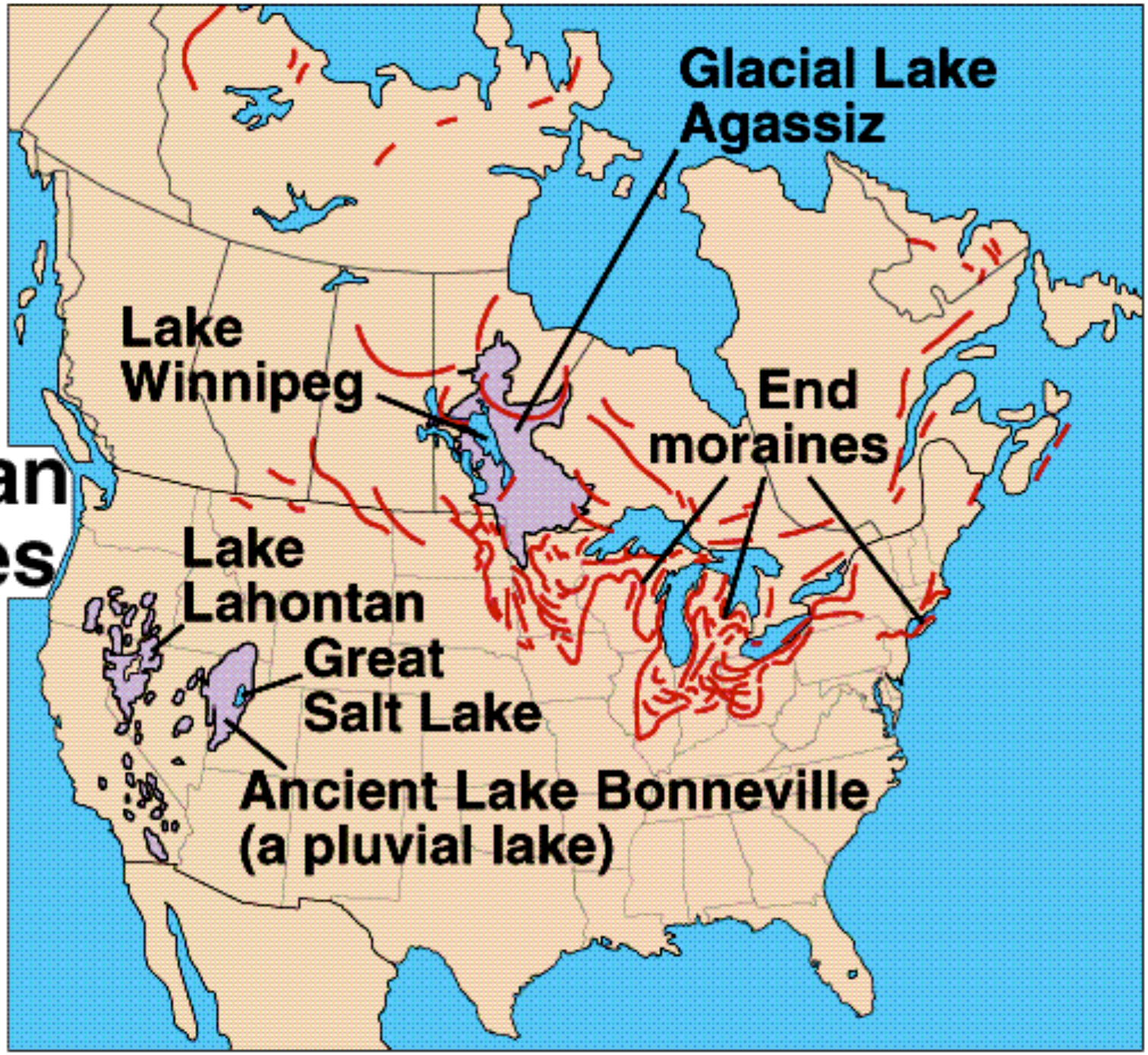

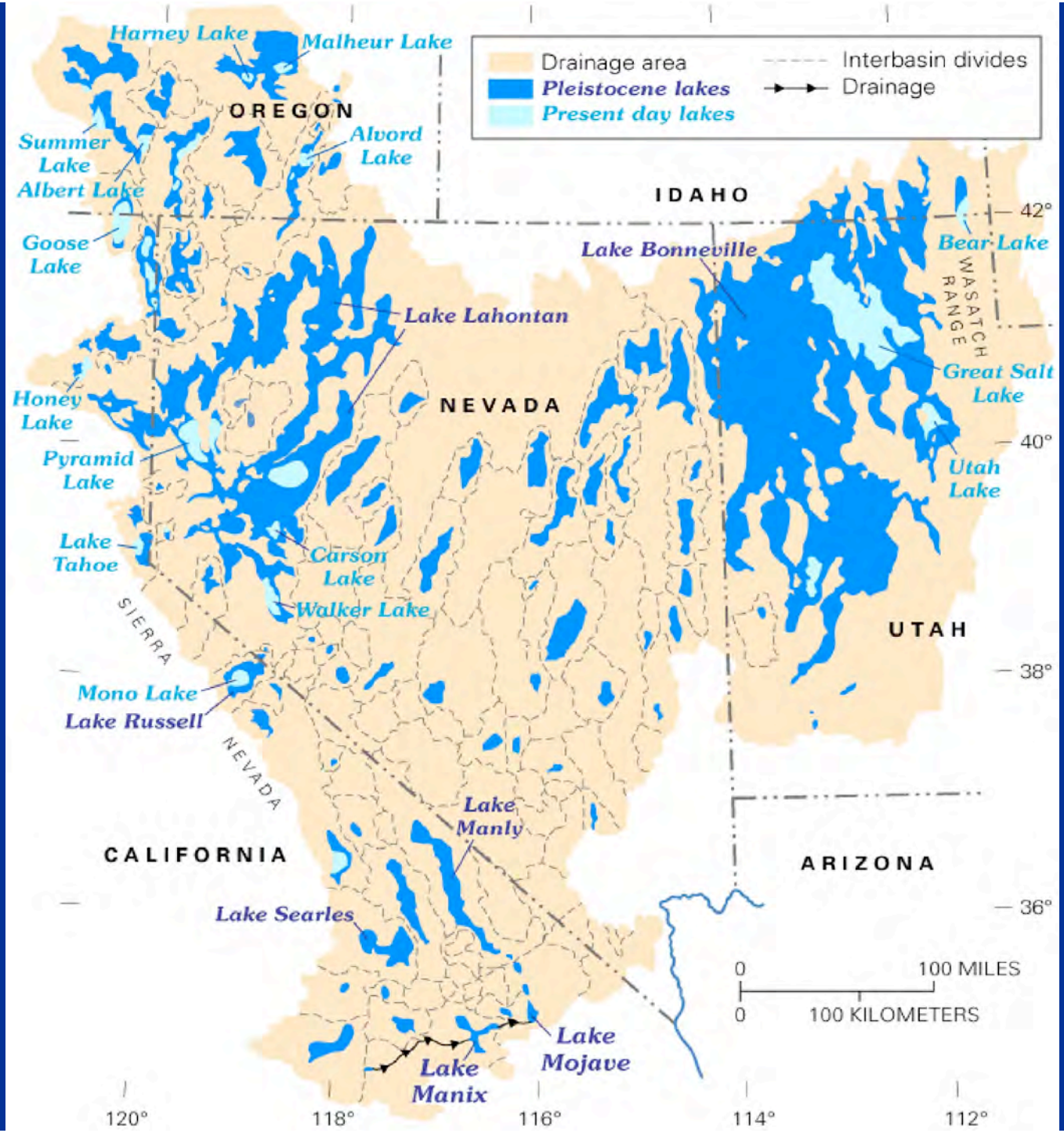
Drainage area
Pleistocene lakes
Present day lakes
Interbasin divides
Drainage
Harney Lake
Malheur Lake
OREGON
Summer Lake
Albert Lake
Alvord Lake
IDAHO
Goose Lake
Lake Bonneville
Bear Lake
WASATCH RANGE
Lake Lahontan
Great Salt Lake
Honey Lake
NEVADA
Pyramid Lake
Utah Lake
Lake Tahoe
Carson Lake
Walker Lake
UTAH
SIERRA NEVADA
Mono Lake
Lake Russell
Lake Manly
CALIFORNIA
ARIZONA
Lake Searles
Lake Mojave
Lake Manix
42°
40°
38°
36°
120°
118°
116°
114°
112°
0 100 MILES
0 100 KILOMETERS

Lake Manly Salt Flats, Death Valley, CA

Lake Bonneville Salt Flats, Nevada-Utah

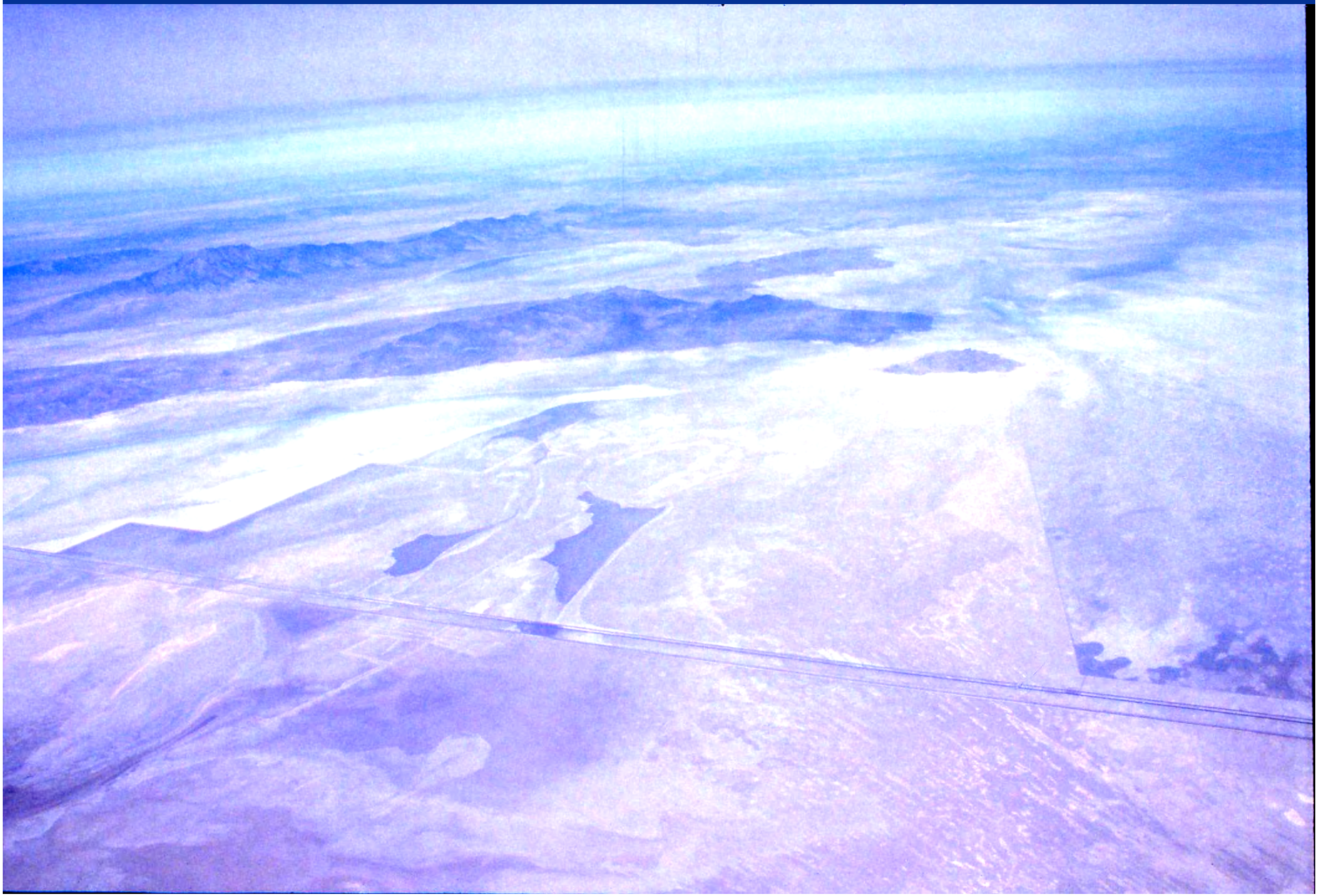

Pyramid Lake, NV

Pyramid Lake, Nevada: Where was Lake Lahontan highstand?

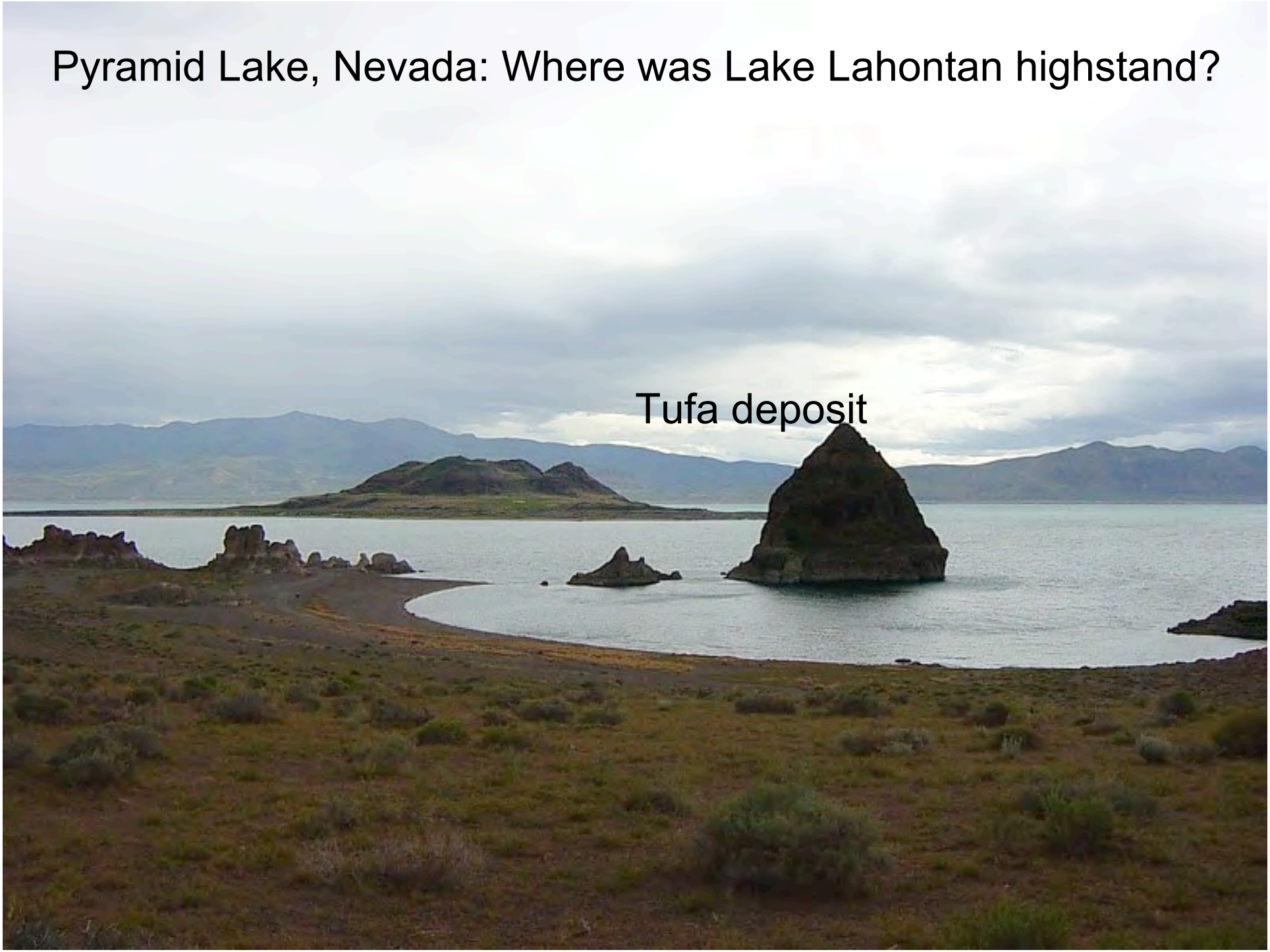

Summer Lake, Oregon

http://commons.wikimedia.org/wiki/File:Summer_Lake_(Oregon).jpg

Summer Lake Basin, Oregon


Albert Lake, Hart Mountain, Oregon

Steens Mountain, Alvord Lake Basin, Oregon

Alvord Playa, east of Steens Mountain


Alvord Lake, Oregon

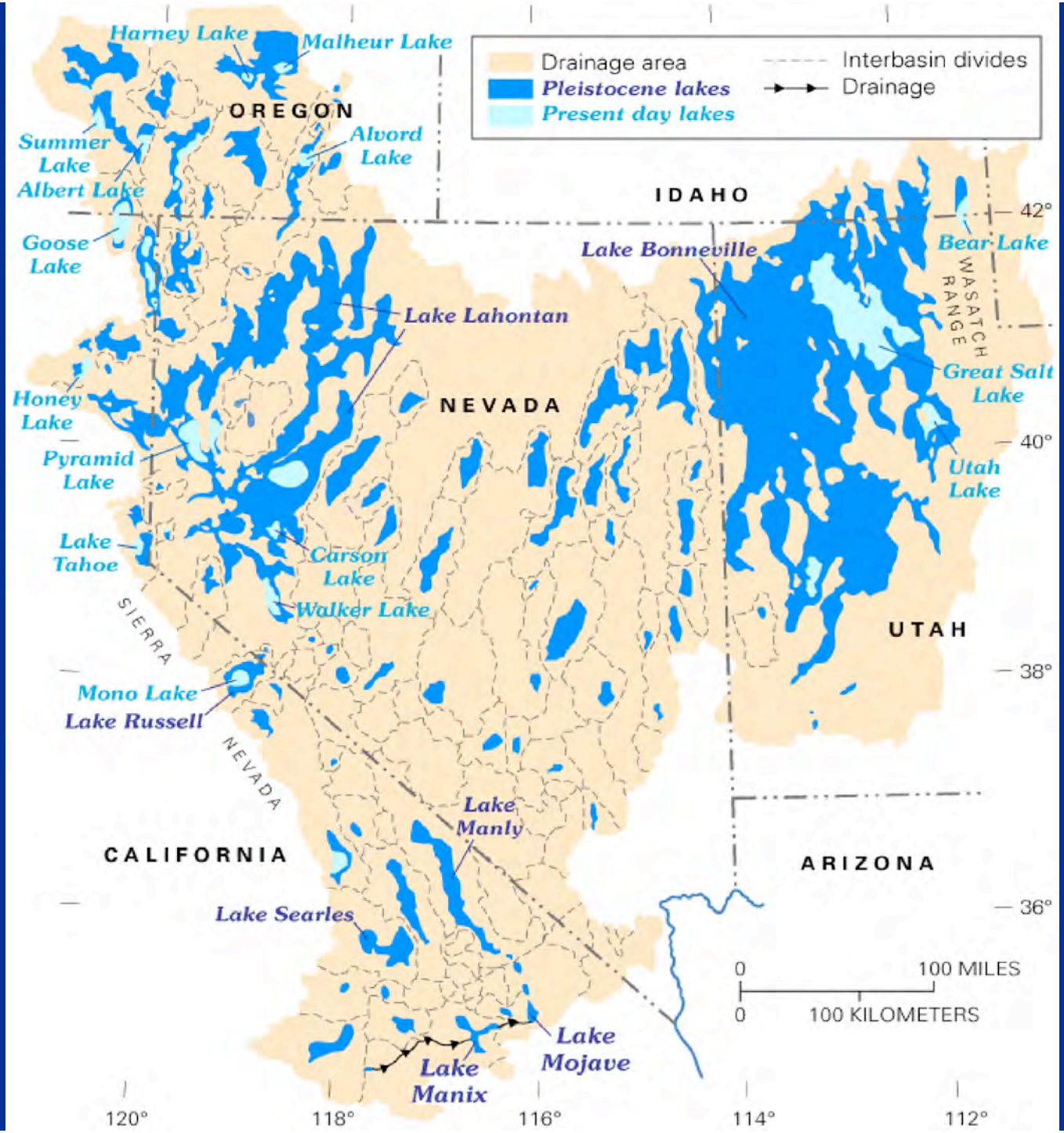
Drainage area
Pleistocene lakes
Present day lakes
Interbasin divides
Drainage
Harney Lake
Malheur Lake
OREGON
Summer Lake
Albert Lake
Alvord Lake
IDAHO
Goose Lake
Lake Bonneville
Bear Lake
WASATCH RANGE
Lake Lahontan
Great Salt Lake
Honey Lake
NEVADA
Pyramid Lake
Utah Lake
Lake Tahoe
Carson Lake
Walker Lake
UTAH
SIERRA NEVADA
Mono Lake
Lake Russell
Lake Manly
CALIFORNIA
ARIZONA
Lake Searles
Lake Mojave
Lake Manix
42°
40°
38°
36°
120°
118°
116°
114°
112°
0 100 MILES
0 100 KILOMETERS

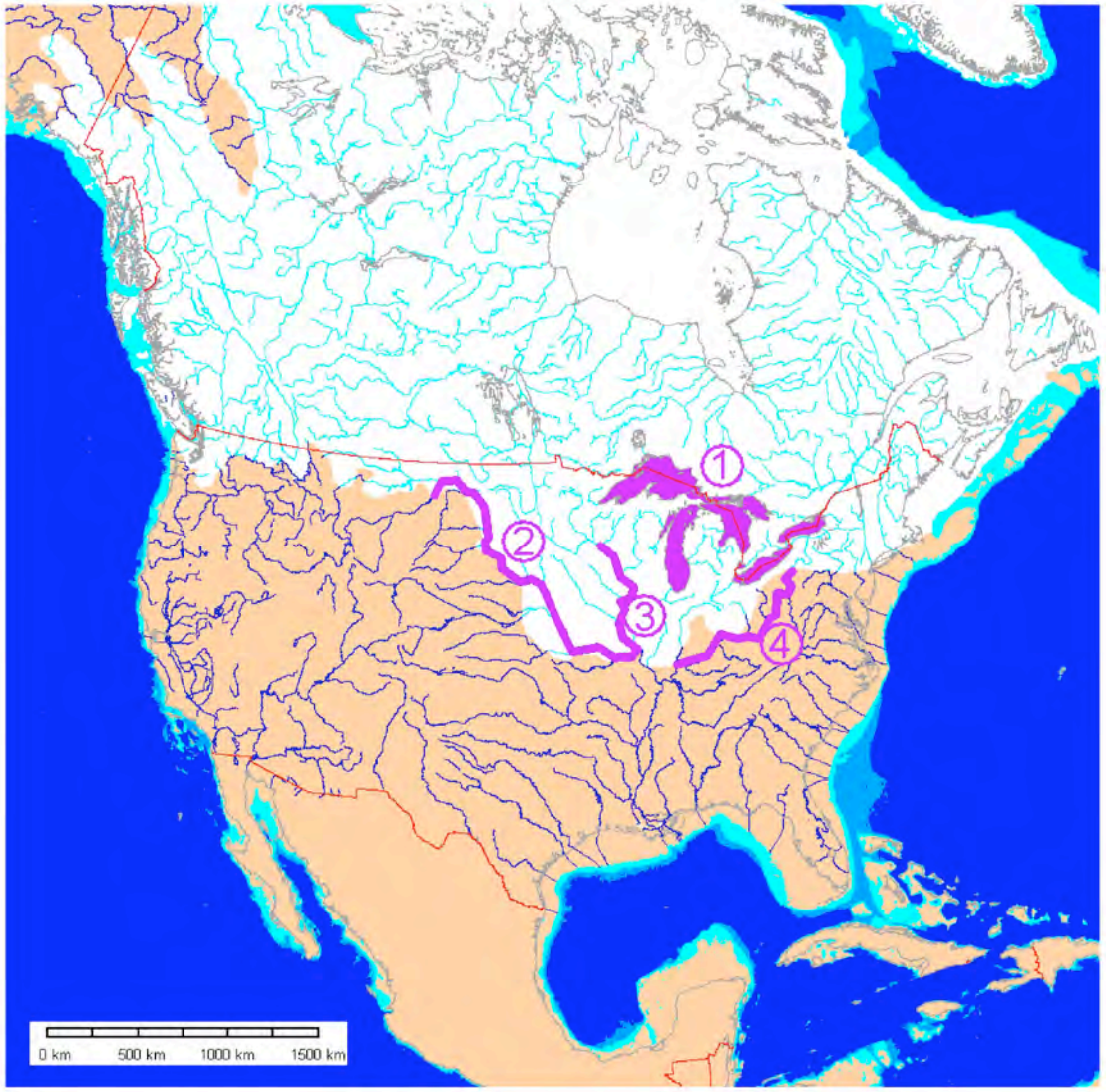

Glacial Maximum North America

Major Effects:

1. Great Lakes
2. Missouri River Drainage
3. Upper Mississippi River Drainage
4. Ohio River Drainage

Columbia Ice Sheet at glacial maximum.
Area of Missoula Flood inundation

Somewhere well above the river . . .

. . . We find a deposit of young, unconsolidated sediments . . .


. . . Which are not derived from local sources.

Nearby, one must ask: Where is the soil?


Well upstream of the Dallas . . . Wallula Gap, WA-OR


Intervals of clean rock all along the Columbia River

Dry Falls, Washington

Pacific Northwest and the "Missoula Floods"

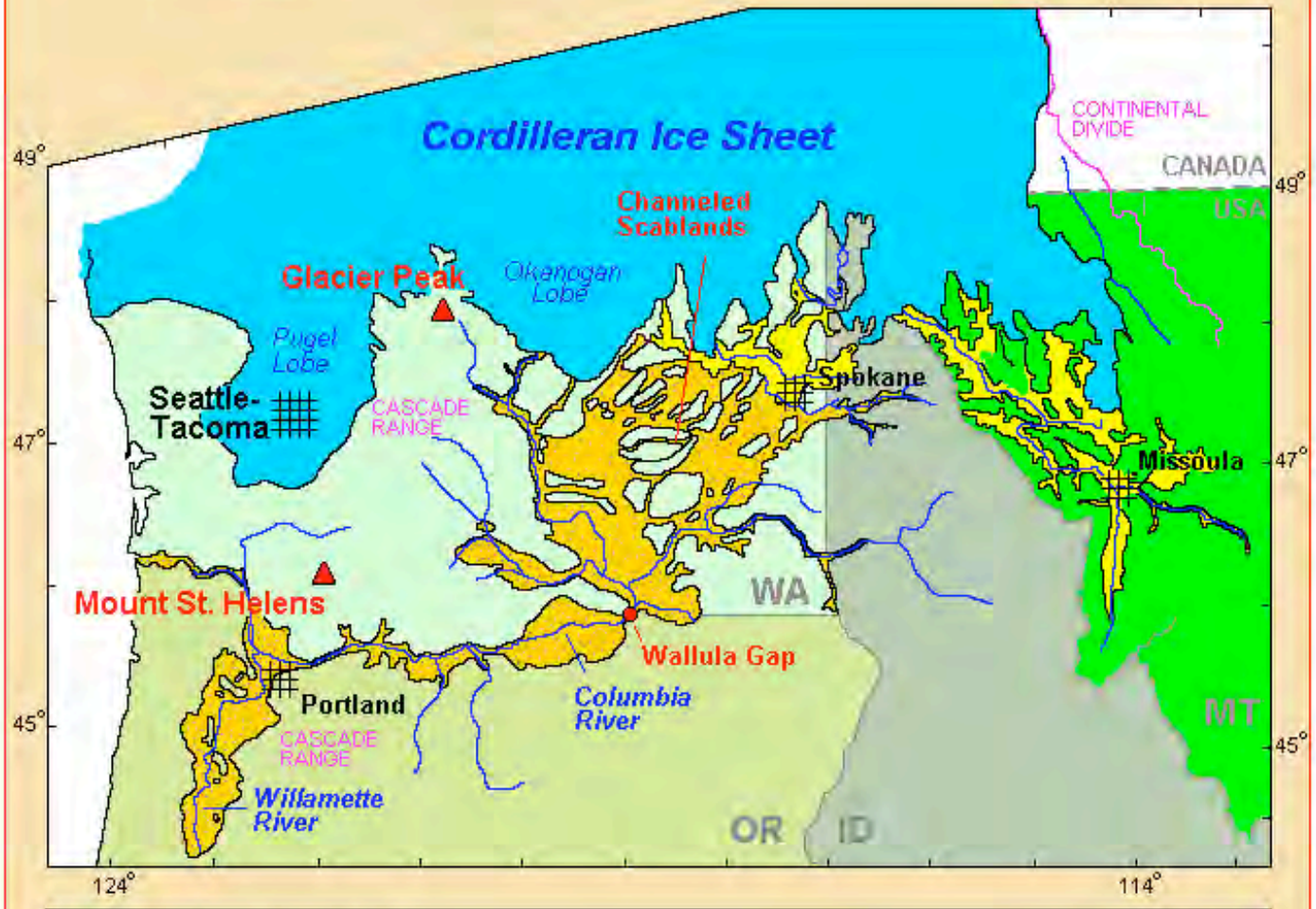

Cordilleran Ice Sheet

Maximum extent of Glacial Lake Missoula (eastern) and Glacial Lake Columbia (western)

Areas swept by Missoula and Columbia Floods

0 100 miles

0 200 kilometers

USGS

Topinka, USGS/CVO, 2002; Modified from: Waitt, 1985

Missoula Flood

Innundation

Depths,

Willamette

Valley

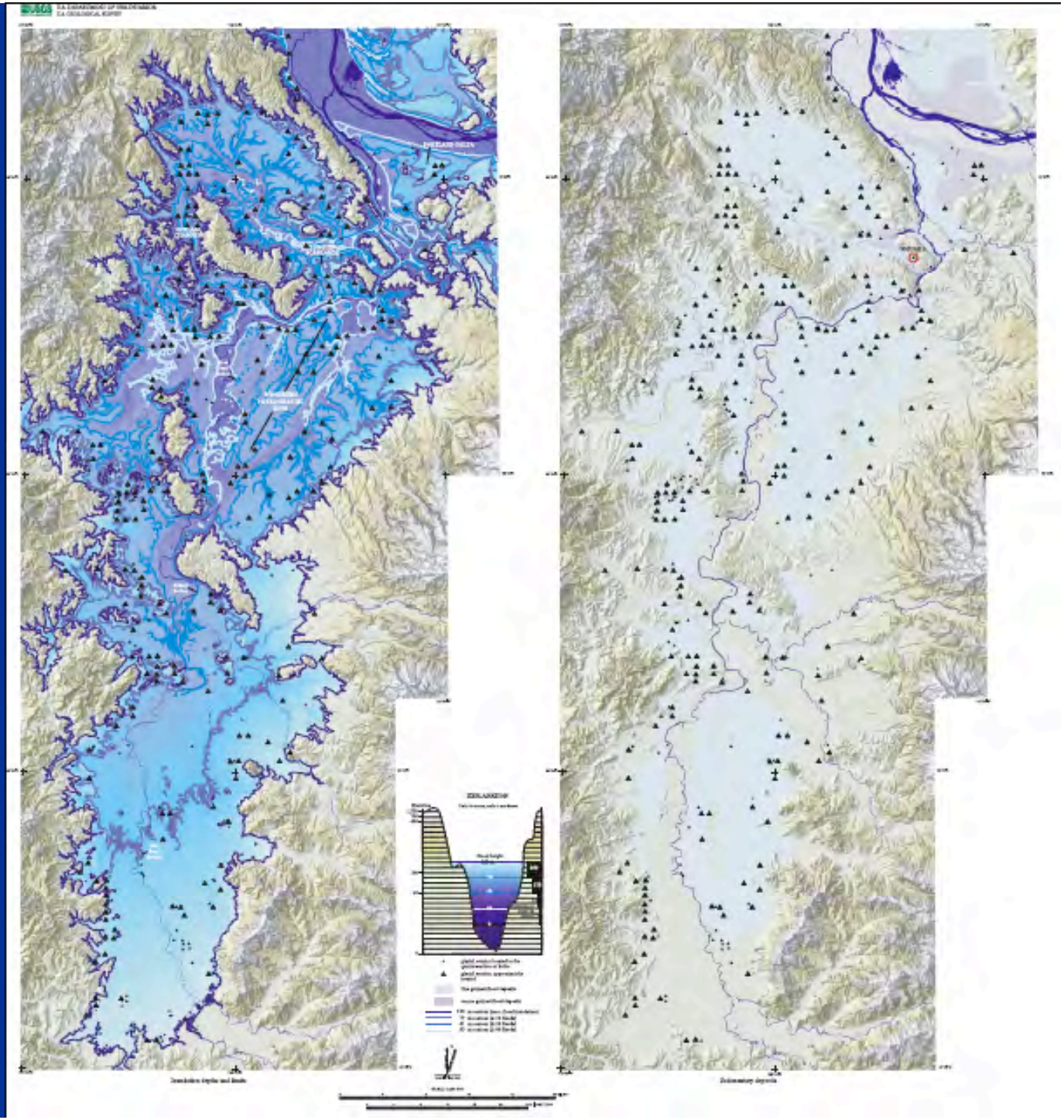

TABLE 1. RESULTS OF DIFFERENT INITIAL AND BOUNDARY CONDITION SCENARIOS

Scenario name	Initial conditions: Southern ice-sheet margin	Initial conditions: Lake Missoula surface elevation (m)	Initial conditions: Base-flow conditions	Initial conditions: Great bend of Columbia (northwest reach)	Grid spacings (m)	Objectives	Outcomes
Initial ice position	20 km north of upper Columbia channel (Grand Coulee to Spokane)	1200	Dry	Open	450	Floodwater travel times through Columbia and Scablands	Columbia flooding lags overland flow; Pasco takes 50 h or more to fill. Columbia path flow times are too long to create maximum stage.
Initial ice position	10 km north of upper Columbia channel	1200	Discharge of ~1000 m^3/s throughout Columbia channels	Closed west of Grand Coulee	450	Grand Coulee and Scablands travel times; influence of ice limit north of the upper Columbia	Grand Coulee flooding matches overland flow travel times over Cheney Palouse. Pasco basin fills in about 40 h.
Columbia gorge conveyance testing	N/A	N/A	Sustained 300 m water-surface elevation at Wallula Gap	N/A	450 320 250	Determine grid spacing needed for full conveyance in Columbia gorge	Conveyance increased when node spacing was decreased from 450 m to 320 m; decrease of node spacing from 320 m to 250 m produced negligible increase.
Final	5–10 km north of upper Columbia channel	1250	Max of 10,000 m^3/s throughout Columbia channels	Closed west of Grand Coulee	250	Determine peak stages from ice dam to Crown Point, maximum stream power, travel times, and time to drain Pasco basin	Fit all contemporaneous peak-stage indicators from Wallula Gap to Crown Point; 3 wk required to drain to the ocean; and peak stream power is consistent with distribution of channel landforms.

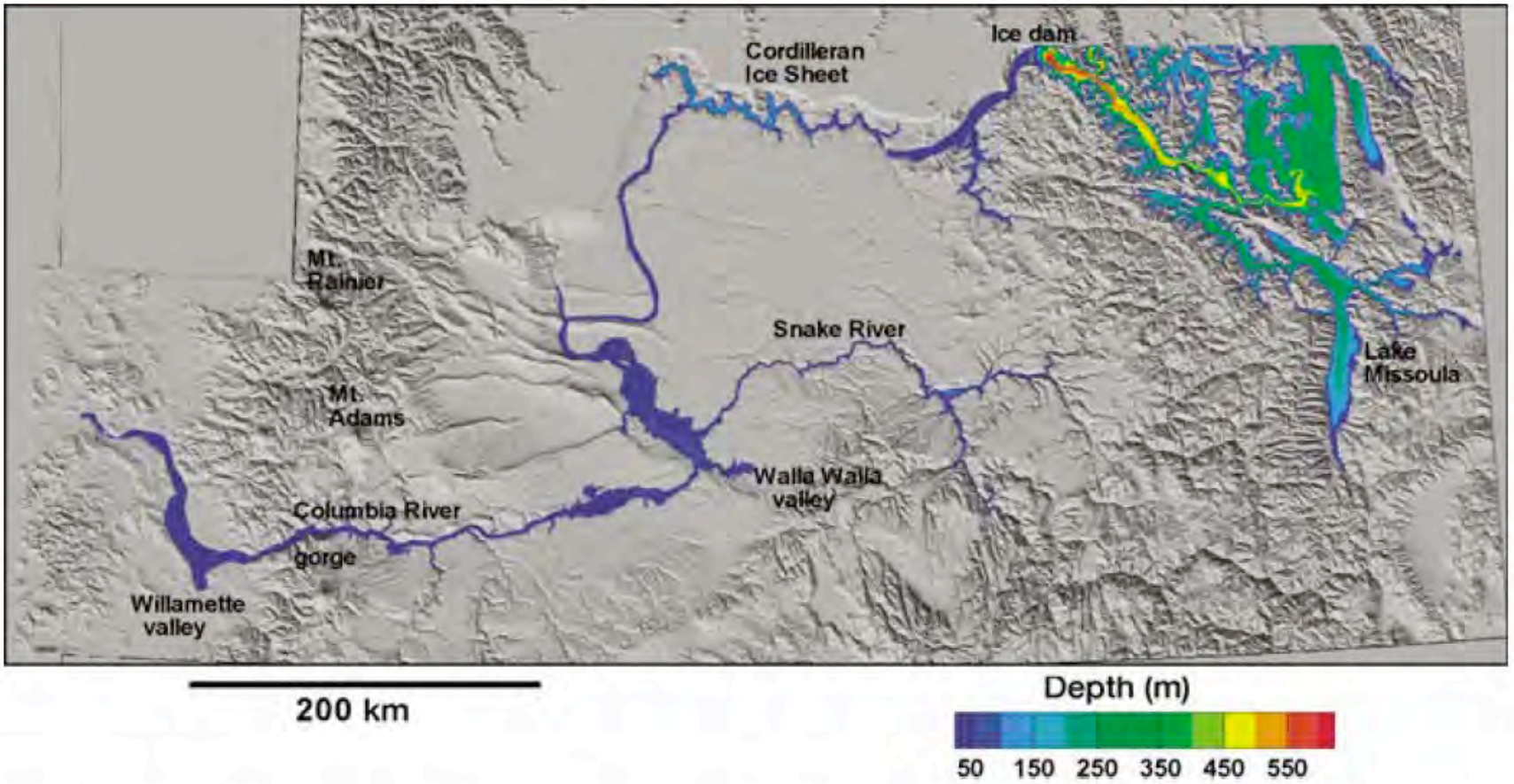

Figure 2. Initial conditions for our Missoula flood simulation. A model of Glacial Lake Missoula was formed by damming the Clark Fork of the Columbia River at the location labeled "ice dam." We experimented with various terminus positions for the continental ice sheet during Fraser glaciations ca. 14,000 radiocarbon yr B.P. to simulate various configurations that blocked and confined the Columbia River channel (Table 1). A constant terminus latitude north of Lake Missoula caused a small additional arm of Lake Missoula in the northeast, but this did not affect routing of flows. We used a base flow in the Columbia River system at the time of dam rupture ranging from dry to a maximum of 10,000 m^3/s (350,000 ft^3/s), or one-third of the flow that was measured in the gorge during the flood of 1894.

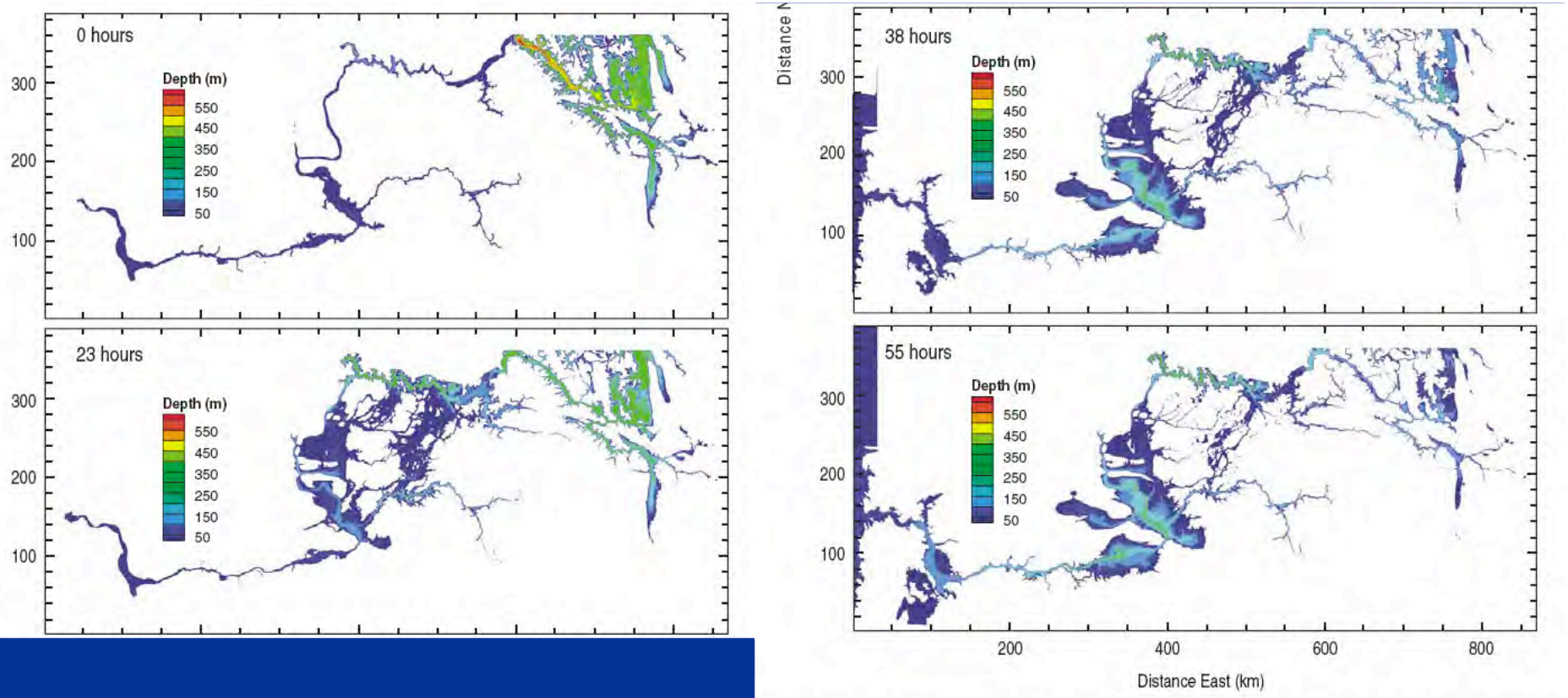

Figure 3. Flooding of eastern Washington from catastrophic rupture of the ice damming Glacial Lake Missoula was rapid and severe. Maximum inundation of the Channeled Scablands occurs 23 h after dam rupture, and this overland flow begins filling Pasco Basin a full day before flow is developed throughout the remainder of the Columbia River drainage system. Pasco Basin achieves maximum stage 38 h after dam break occurs, and maximum stage in Umatilla Basin and Walulla Gap (see Fig. 1) follows 17 h later.

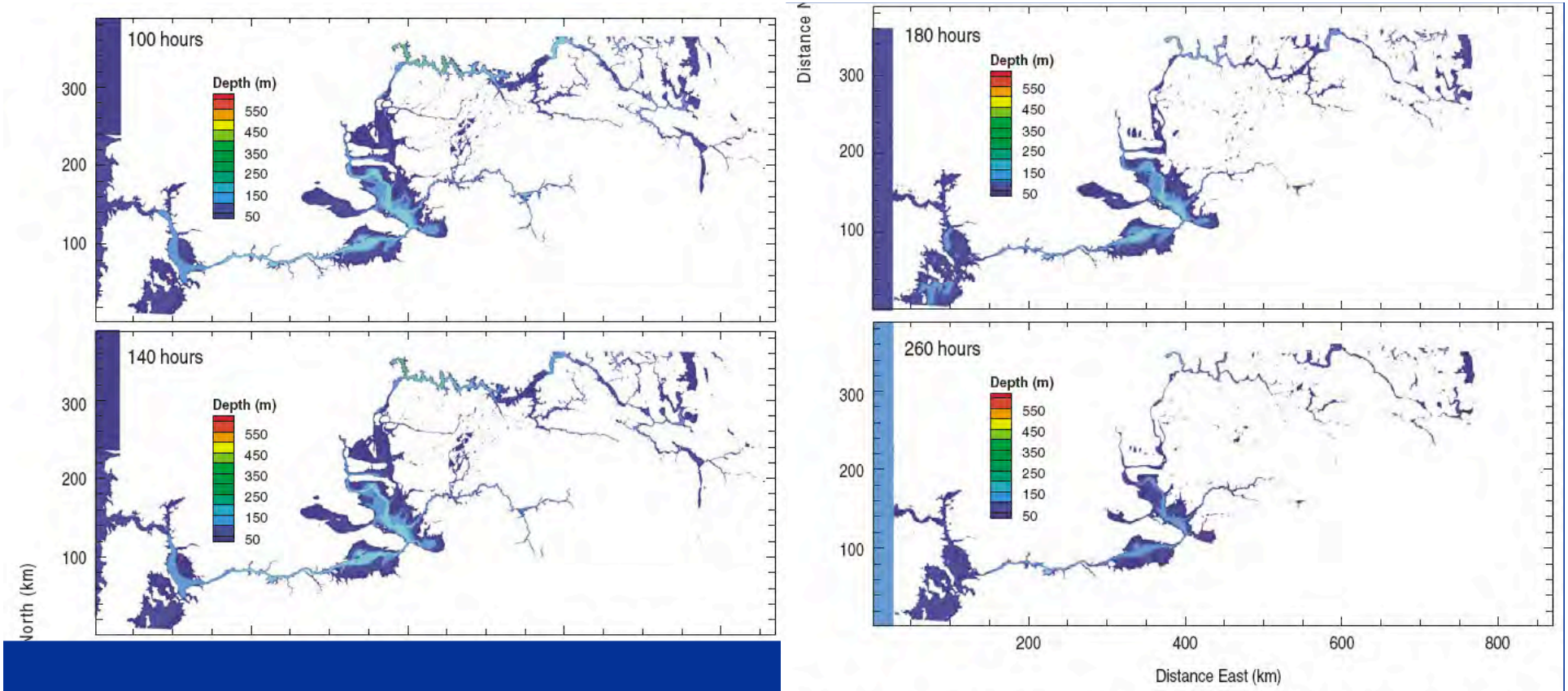

Figure 5. Drainage of Glacial Lake Missoula and the upper Columbia River system during a large Missoula flood. The broad basins of Pasco, Yakima, and Umatilla drain through Columbia gorge, extending the duration of flooding to 325 h. This long duration is primarily caused by the discharge limitation of the gorge, and secondarily by low gradients from the Willamette Valley to the Pacific Ocean in the final stages of flow.

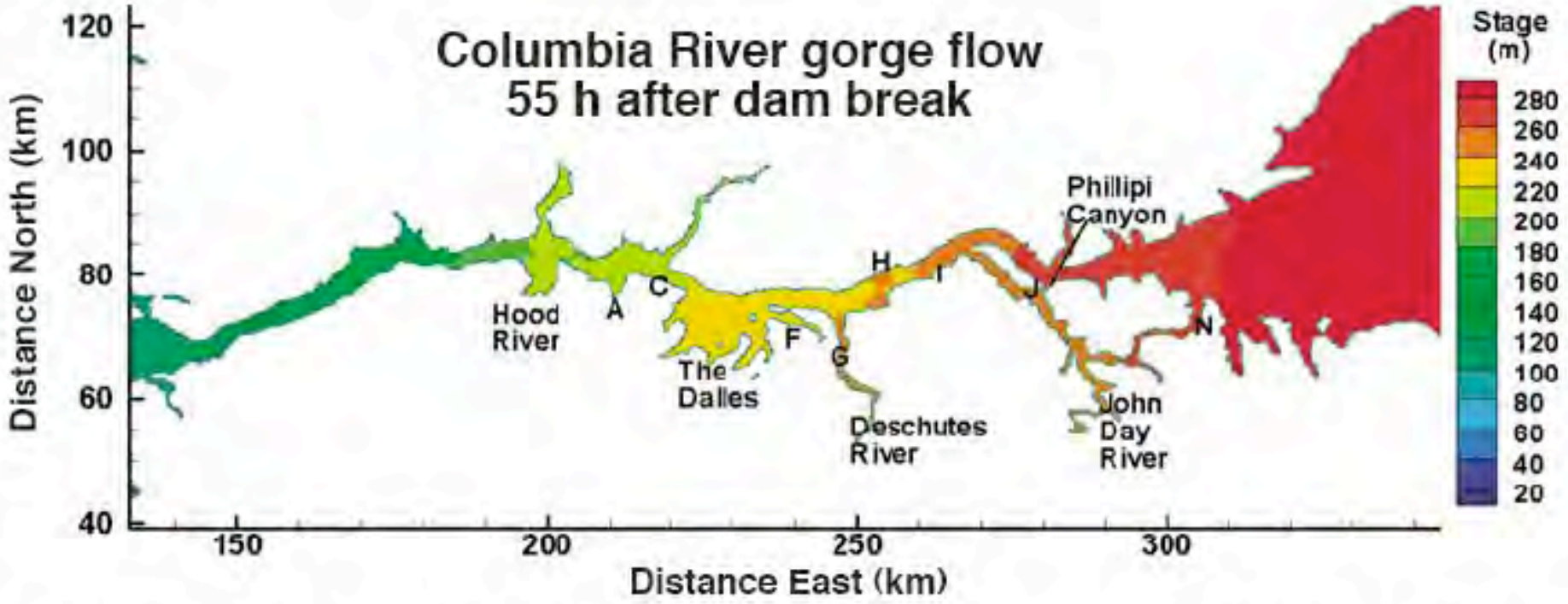

Figure 10. Flood stage west of Umatilla Basin 55 h after dam break when the flood stage of Umatilla Basin is at peak. Letters correspond to field locations in Benito and O'Connor (2003) that are compared to model output in Table 5.

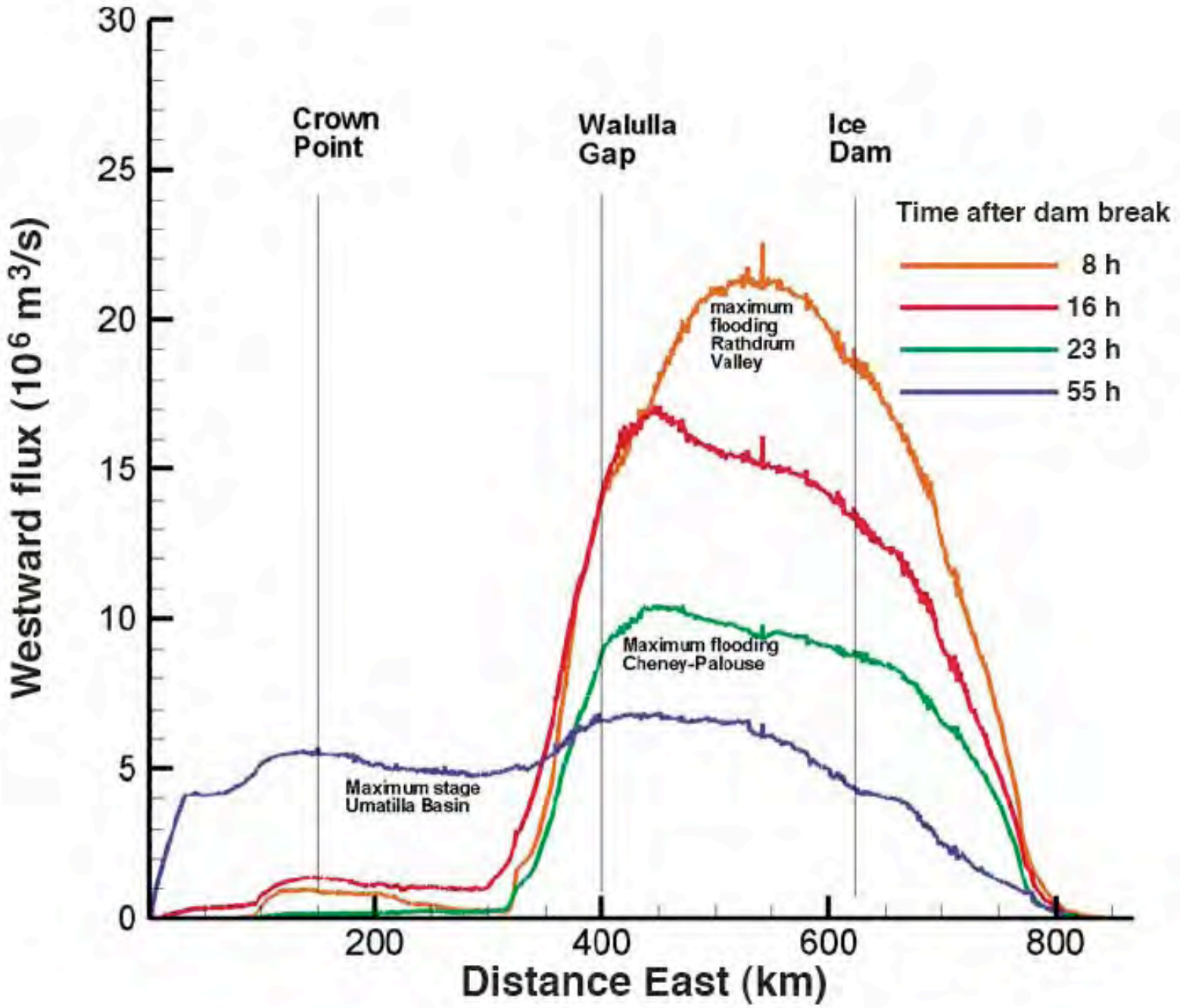
Crown Point
Walulla Gap
Ice Dam
Time after dam break
8 h
16 h
23 h
55 h
maximum flooding Rathdrum Valley
Maximum flooding Cheney-Palouse
Maximum stage Umatilla Basin
Westward flux (10^6 m^3/s)
Distance East (km)
0
5
10
15
20
25
30
200
400
600
800

Hydrologic Cycle - 2% of water is Ice

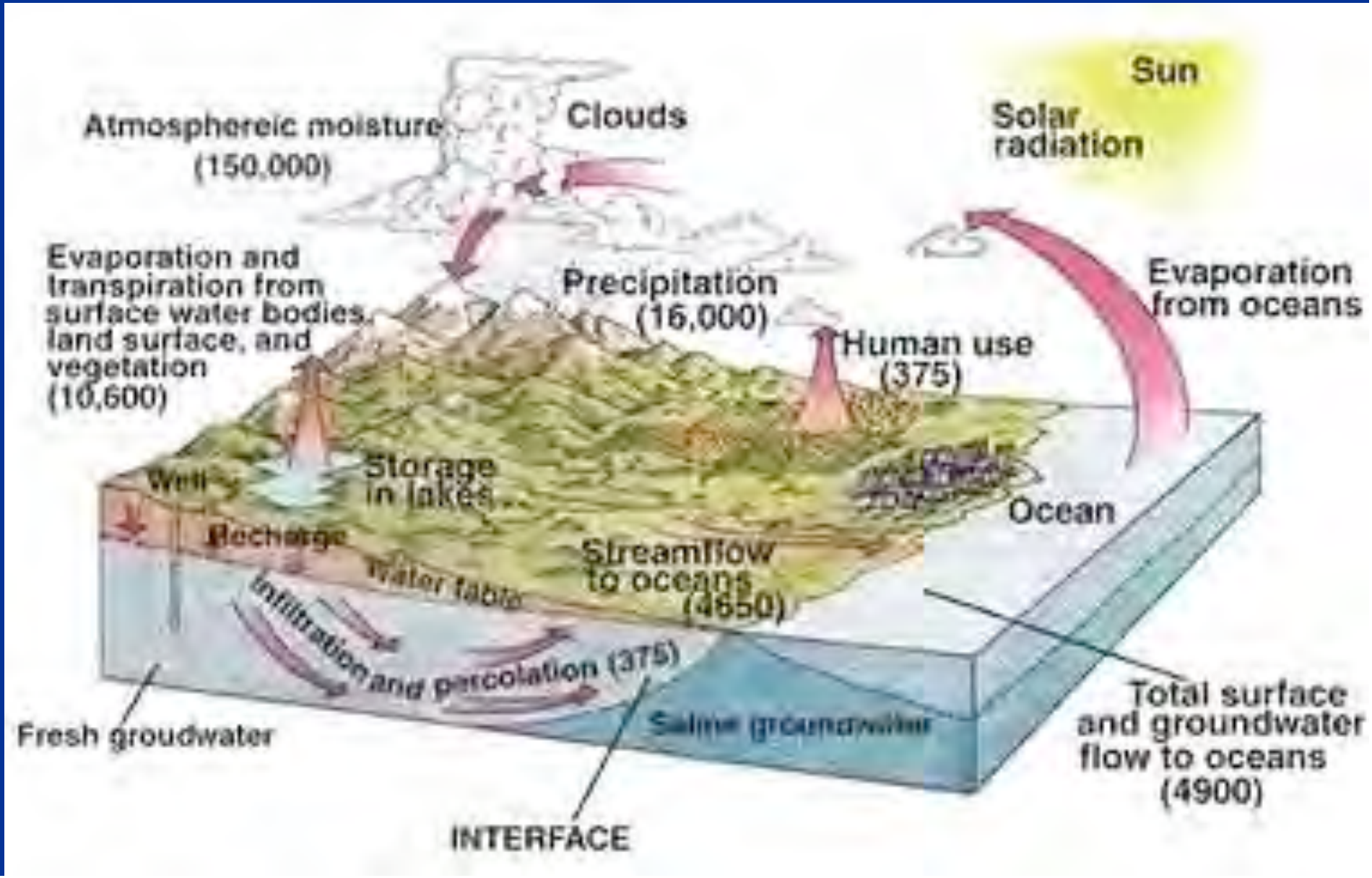

What if the glaciers melt?

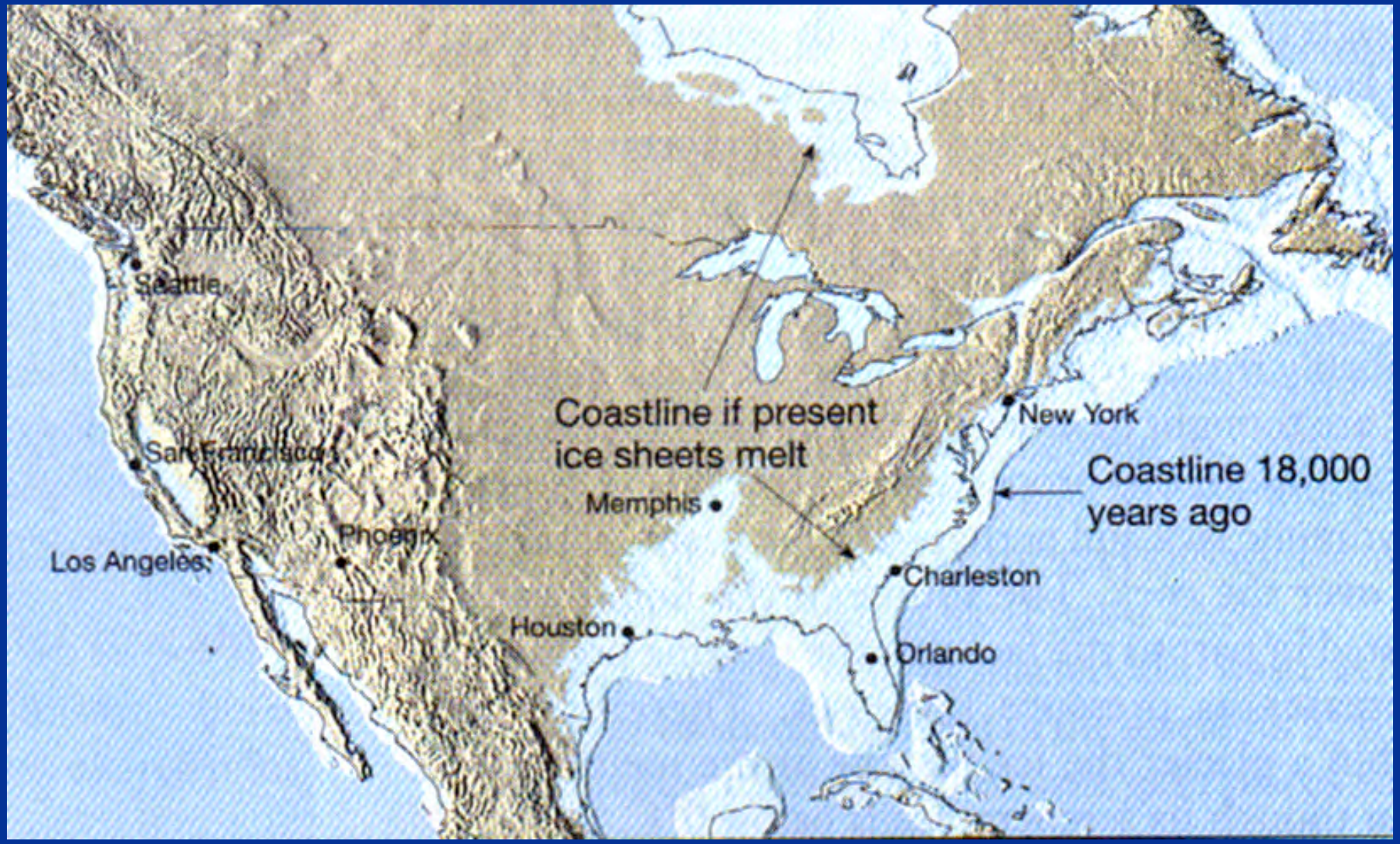

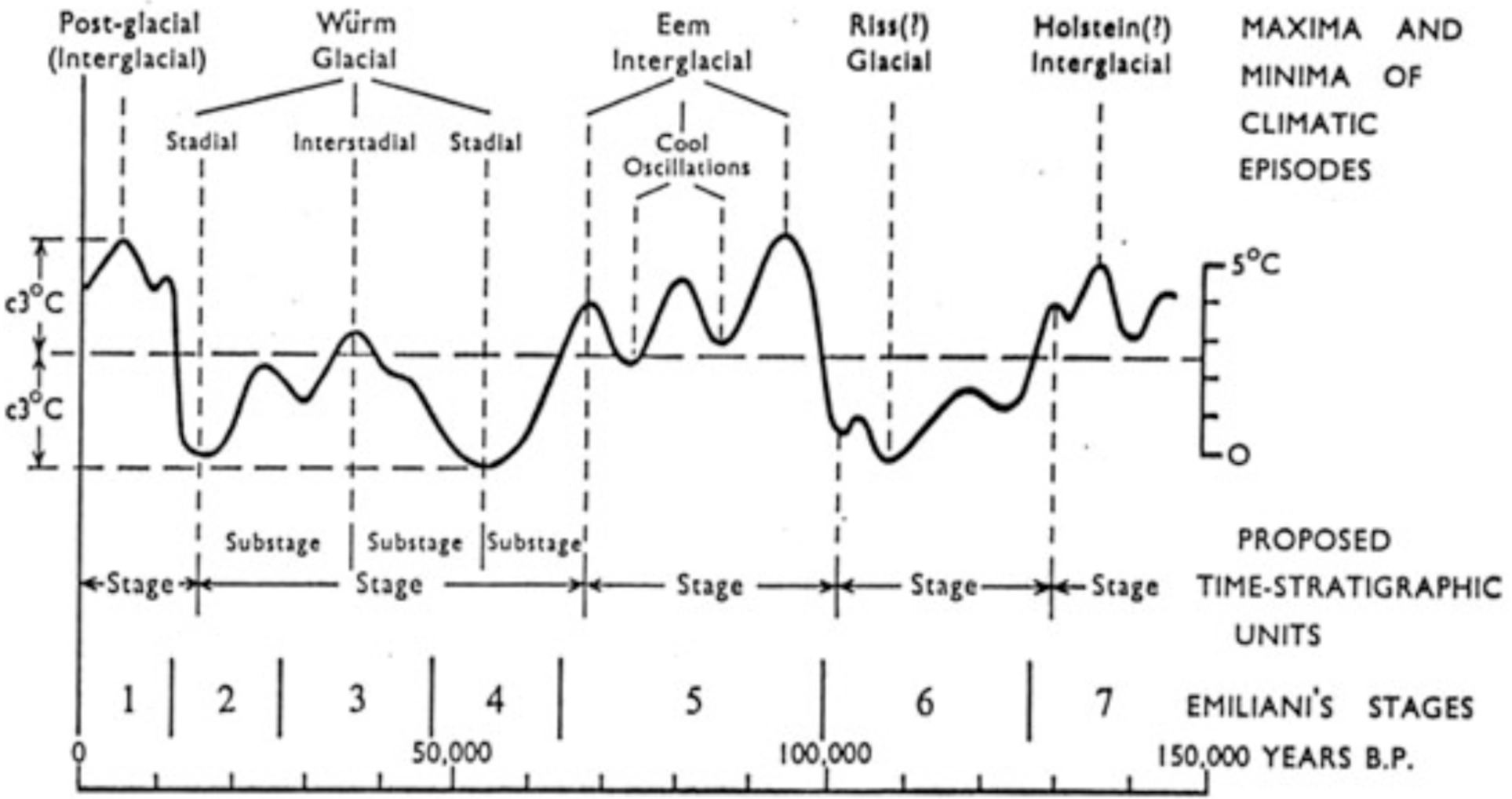

European Quaternary Glacial Stages

What Causes Glaciation?

Major Climatic Forcing Mechanisms of the Sun - Earth Climate System

EXTERNAL

Solar Radiation and Galactic Forcing

- Sunspot variation and irradiance changes
- Solar ultraviolet wavelength variability
- Magnetic variation
- Celestial influence?

Earth's Orbital Changes

- Eccentricity
- Obliquity
- Precession of equinoxes

Asteroid Impacts

- Aerosols
- Extinction

The Moon

- Gravity deflections
- Earth and ocean tides
- Biological rhythms

(Art Green)

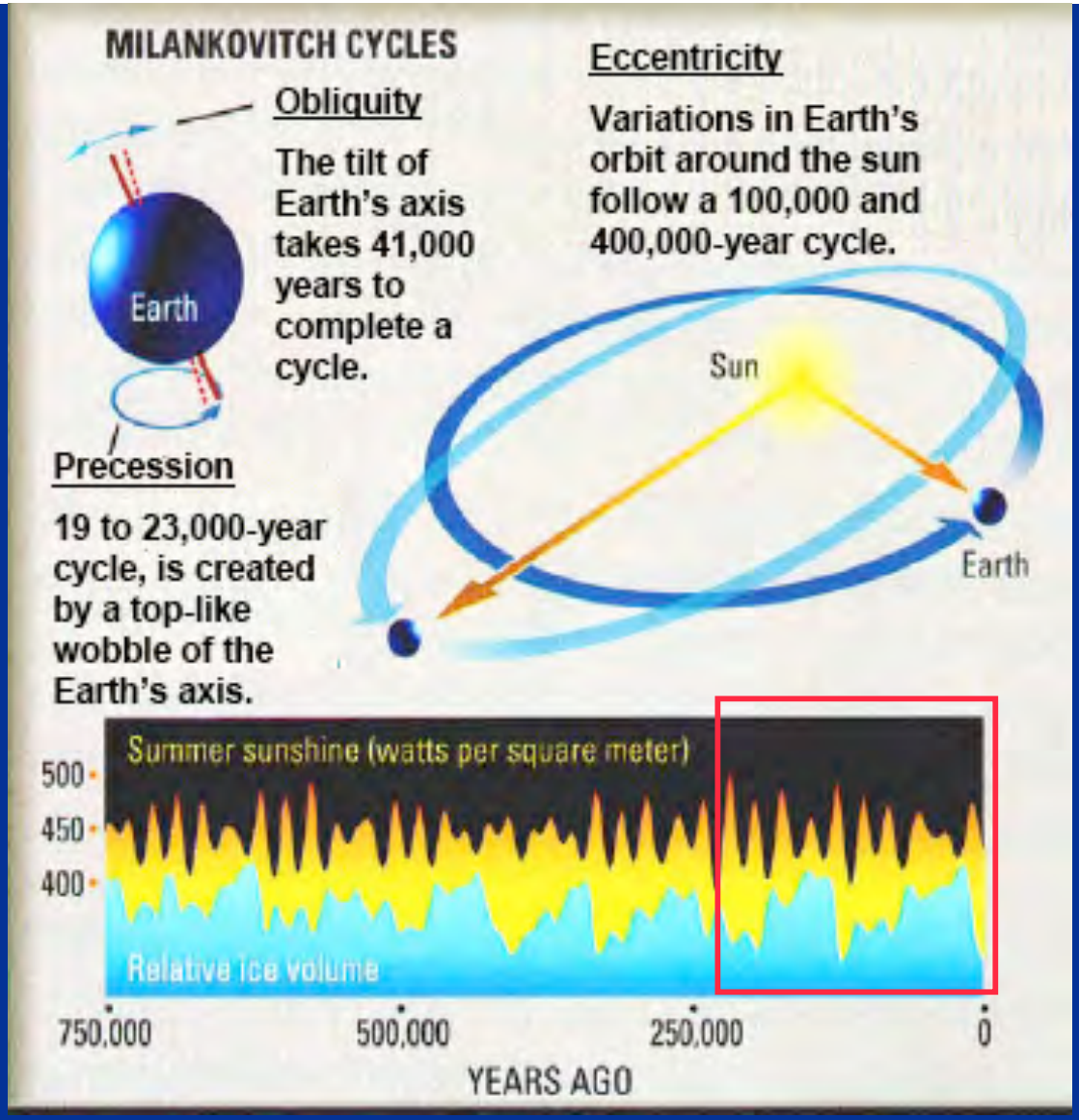

(Art Green)

Earth's Orbital Changes - Linear cycles within a non-linear system

- **Eccentricity - changes in the shape of the orbit about the sun 100K-400k cycles**
- **Obliquity - tilt of the earth (231/2°) 41k cycle**
- **Precession of equinoxes - the timing of the Earth's closest approach to the sun (19k-23k)**

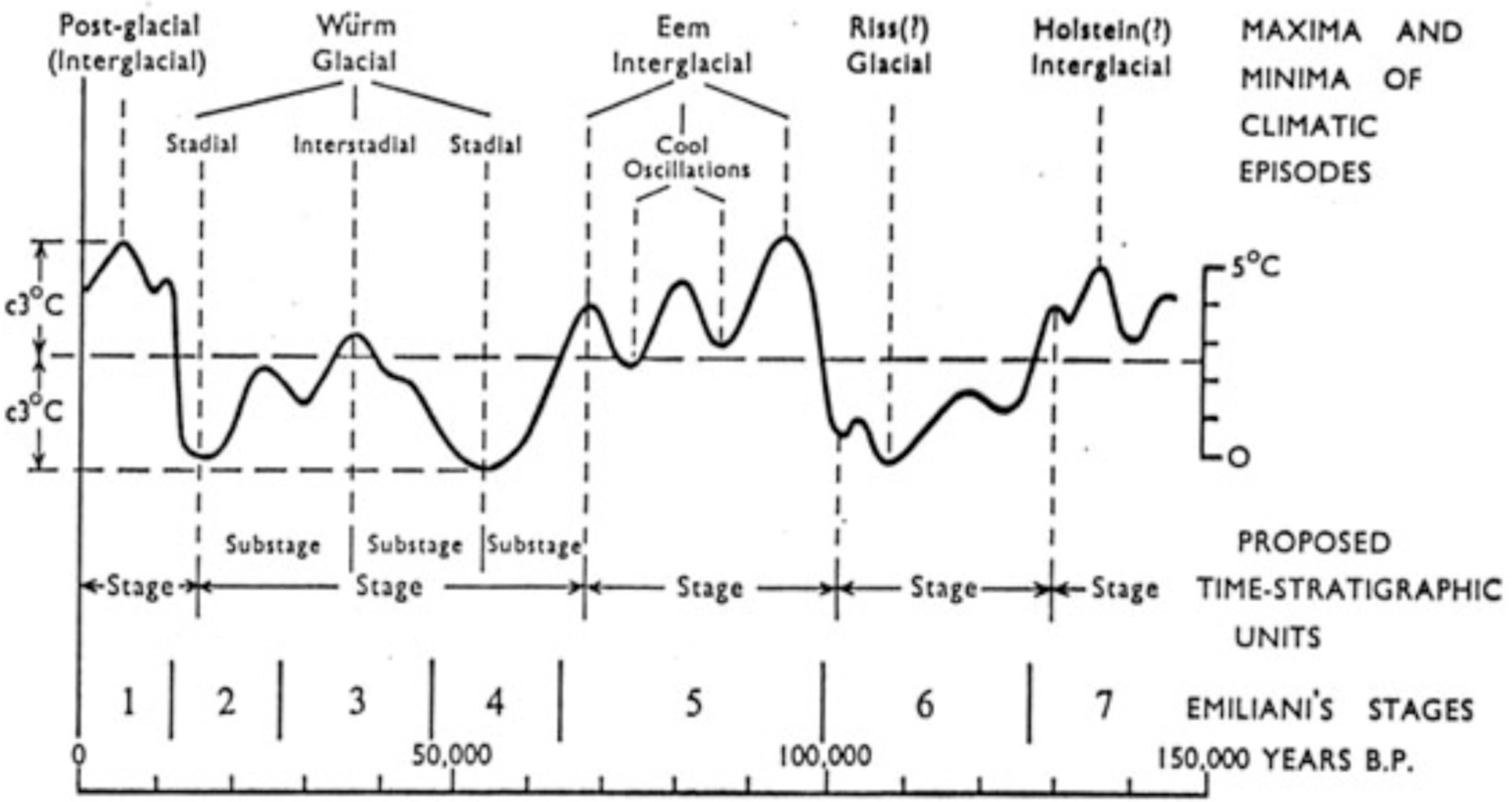

European Quaternary Glacial Stages

Milankovitch Cycles Recorded in the Calatayud Basin of NE Spain

Spectral analyses of proxy records in both the depth and the time domain reveal that the small-scale mudstone-carbonate cycles correspond to the astronomical 19-23 kyr precession cycles, whereas the large-scale cycles reflect the 400 kyr eccentricity cycle.

Abdul Aziz, 2001 / SEDIMENTOLOGY Volume 50, Number 2 / April 2003

Melting Glaciers on Mt Ranier: Climate Change or Weather Anamoly?

Sisson et al 2011

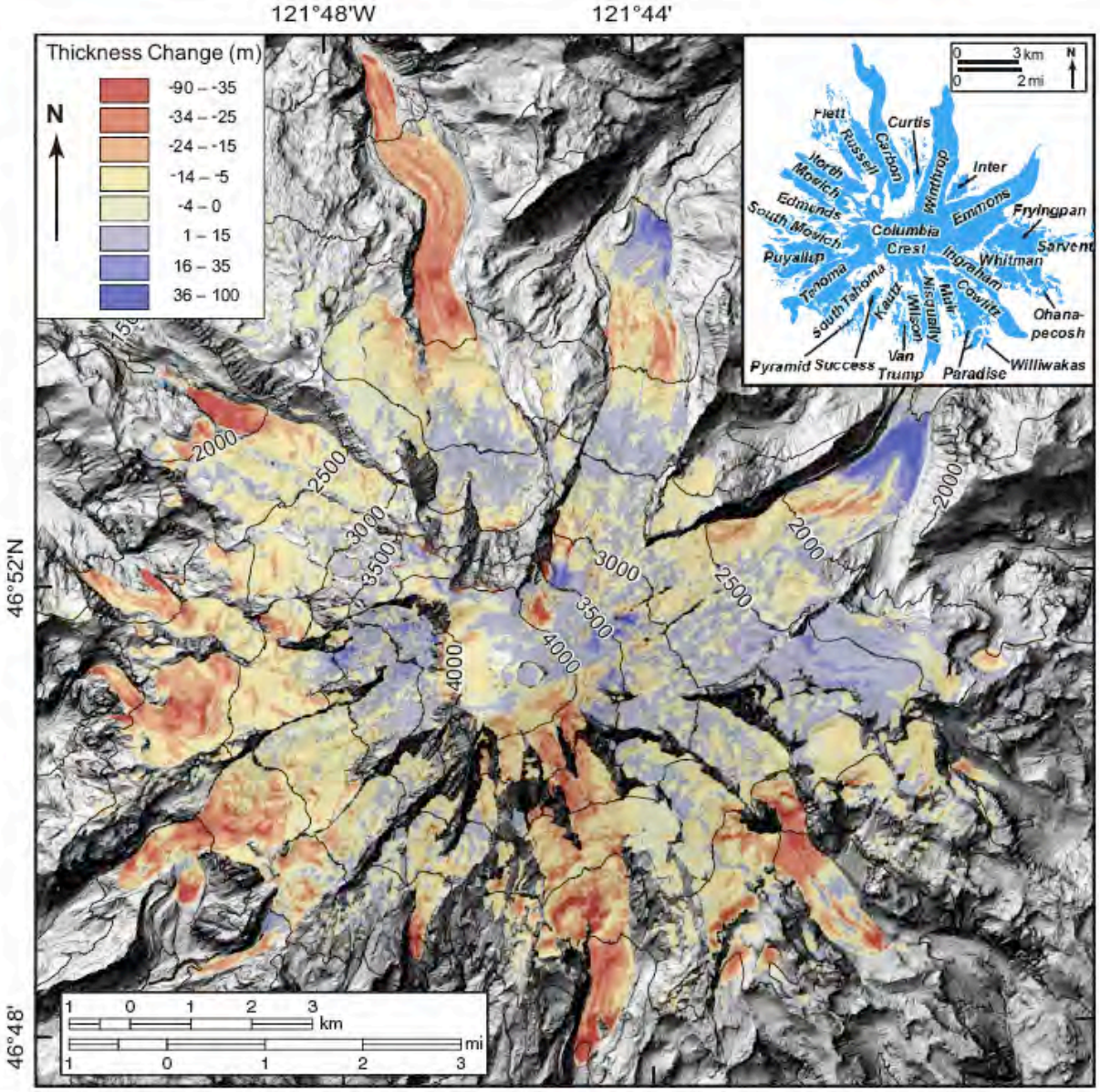

Figure 1. Map of net change in surface elevation of glaciers and snowfields from 1970 to 2007/2008 at Mount Rainier, Washington (colored), derived by digital elevation model (DEM) differencing (see footnote 1). Apparent elevation differences outside of snow- and ice-covered areas are omitted for clarity. Elevation contours (500 m) and background shaded relief are from LiDAR (light detection and ranging) DEM (Robinson et al., 2010). Marginal ticks give north latitude and west longitude. Inset shows index map and names of glaciers and perennial snowfields (blue) at Mount Rainier.

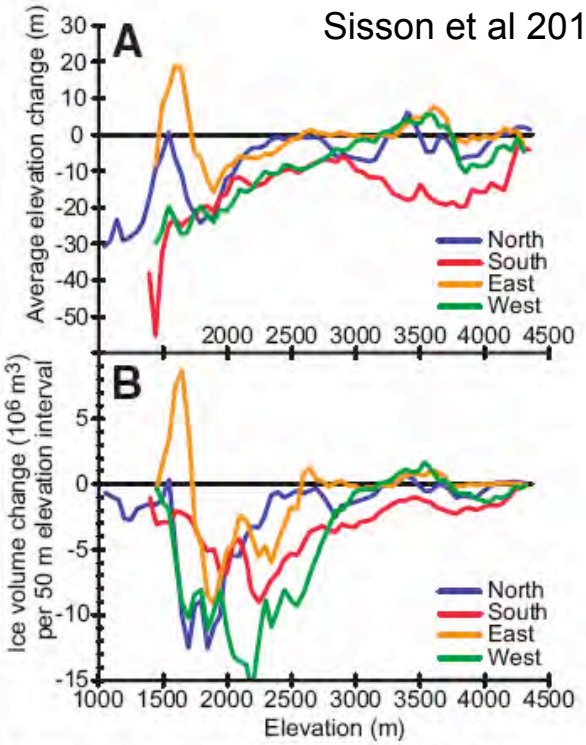

Figure 2. A: Average ice thickness changes 1970 to 2007/2008 versus surface elevation for glaciers and crevassed snowfields grouped by exposure aspect (Table 1) and shown for 50 m altitude interval steps. B: Volume changes. Low-elevation thickness and volume anomalies in north and east sectors are due to terminal thickening of Winthrop and Emmons Glaciers.

nal thickening shows that it behaved similarly to nearly all other glaciers on Mount Rainier and supports the inference that low-elevation thickening was due to insulation by rockfall debris (Driedger, 1986; Nylen, 2004). The Emmons Glacier divides from the Winthrop at ~2800 m elevation and is flanked to the east by the Fryingpan Glacier, which also grew slightly (Table 1).

IMPLICATIONS

Causes of 1970 to 2007/2008 Glacier Volume Changes at Mount Rainier

Glaciers melt mainly because of solar irradiation and ambient temperature during the ablation season, a simple approximation being:

$$\frac{dh}{dt} = aT + b(1-\alpha)\varepsilon, \qquad (1)$$

where h is glacier thickness, t is time, T is temperature above the melting point, ε is the aspect-adjusted solar irradiance, α is albedo, and a and b are constants (Pellicciotti et al., 2005). If Mount Rainier's glaciers were in steady state, and summertime temperatures increased regionally with no changes in irradiance or winter snowfall, this expression would predict that all sides of the mountain would lose ice equally. That south-facing glaciers have thinned more and to higher elevations than those on other flanks, and that ice thickened on many areas of the upper mountain, shows that other factors were involved.

Sisson et al 2011

Preferential melting of south-flank glaciers can alternatively be thought of as a recovery from a precipitation anomaly, just as snowfall melts away fastest on hillsides facing the sun due to their higher ε values. The modest advance of many Pacific Northwest glaciers bracketed between the late 1940s and early 1980s corresponds with generally above average snowfall measured at Paradise on Mount Rainier's south flank (Western Regional Climate Center, http://www.wrcc.dri.edu), and by proxy, as above average river discharges in the region during the snowmelt season (U.S. Geological Survey records, http://waterdata.usgs.gov/wa/nwis/monthly). Since ca. 1976, snowfall and discharge have returned to near long-term average values, and snow and ice melted preferentially on Mount Rainier's south flank due to its greater solar irradiance. Ablation season temperatures at Mount Rainier were not in phase with the period of high-snowfall winters, being generally warmer than historic averages from at least 1920 to 1961, generally cooler than average through 1984, and since fluctuating around the historic mean (Western Regional Climate Center; PRISM, http://www.prism.oregonstate.edu). That differential glacier thinning may be a recovery from a high-precipitation anomaly does not negate long-term temperature increases as the primary cause of glacial retreat since the Little Ice Age (Oerlemans, 2005).

Sisson et al 2011

Sheep Mountain

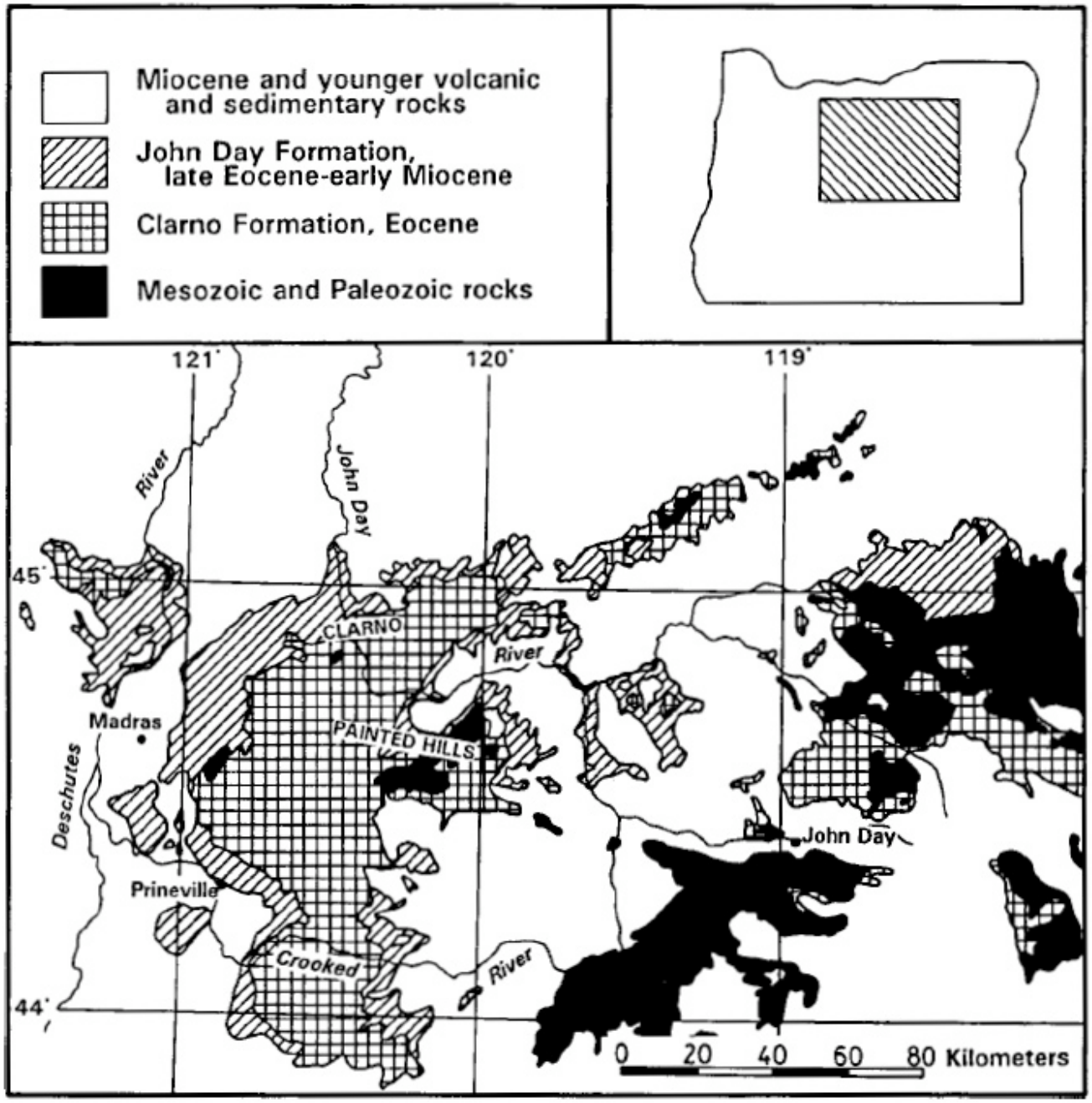

Figure 1. Generalized geologic map of north-central Oregon modified from Walker (1990).

Bestland et al 1996

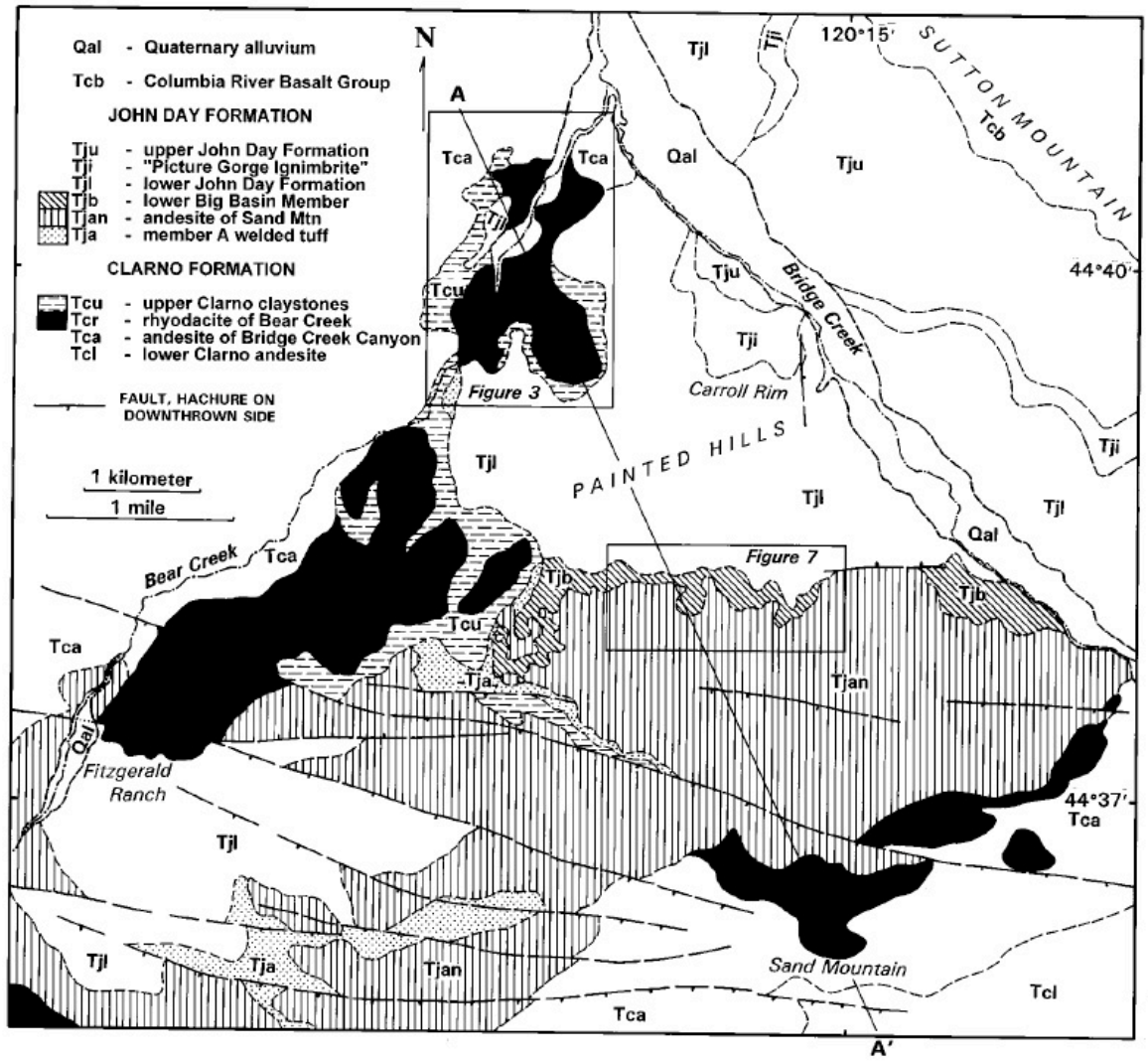

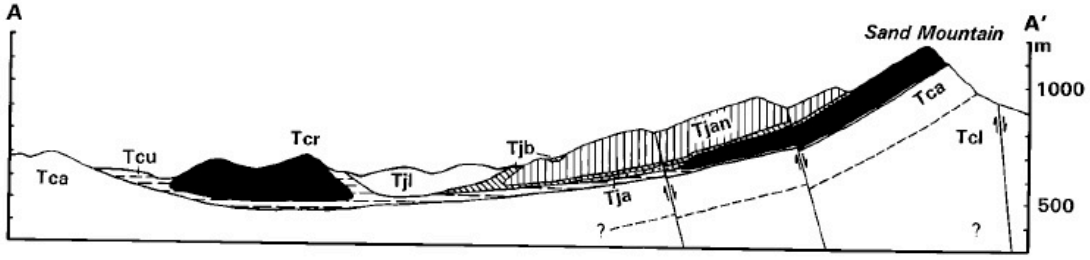

Figure 2. Geologic map of the Painted Hills area and corresponding cross section.

Bestland et al 1996

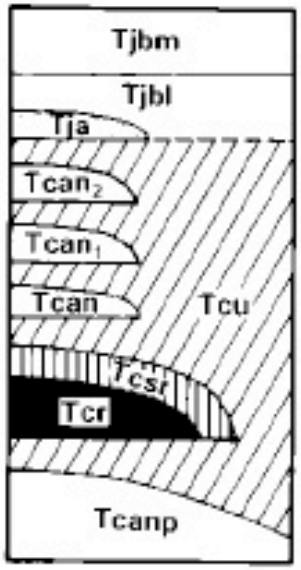

JOHN DAY FORMATION

- Tjbm - Middle Big Basin member
- Tjbl - Lower Big Basin member
- Tja - Welded tuff of member A

CLARNO FORMATION

- Tcu - Red claystones of Brown Grotto
- $Tcan_2$ - Andesite
- $Tcan_1$ - Andesite, plagioclase phyric
- Tcan - Andesite
- Tcsr - Saprolitic platy rhyodacite, minor red claystone
- Tcr - Rhyodacite of Bear Creek
- Tcanp - Andesite of Bridge Creek Canyon

$\overset{\frown}{\sim}_{23}$ Conglomeratic ironstone horizons with strike and dip

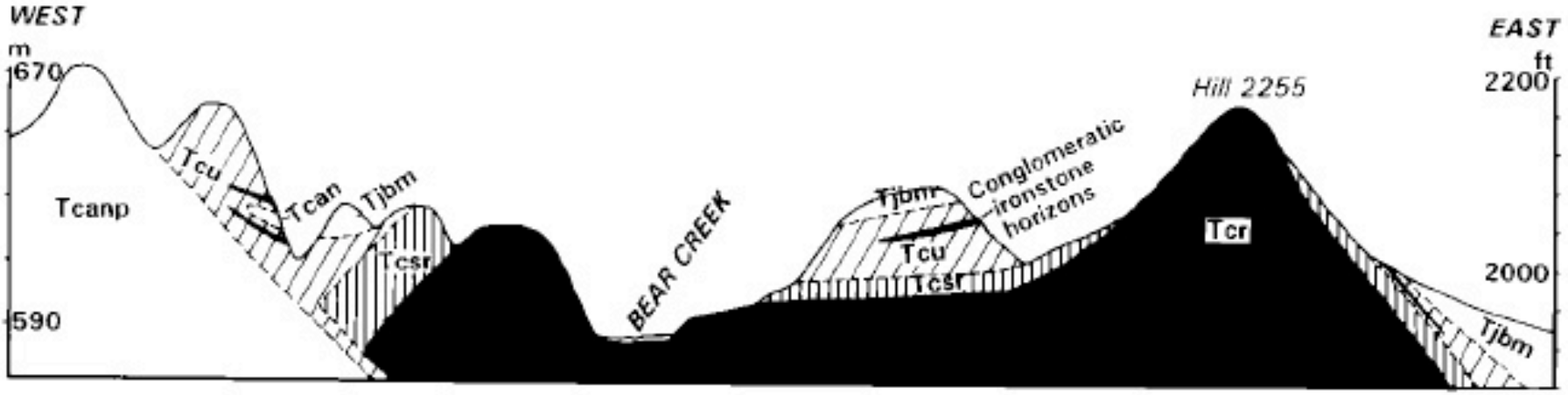

Figure 4. Stratigraphy and cross-section of Painted Cove rhyodacite body.

Bestland et al 1996

(a) Generalized lateritic regolith profile

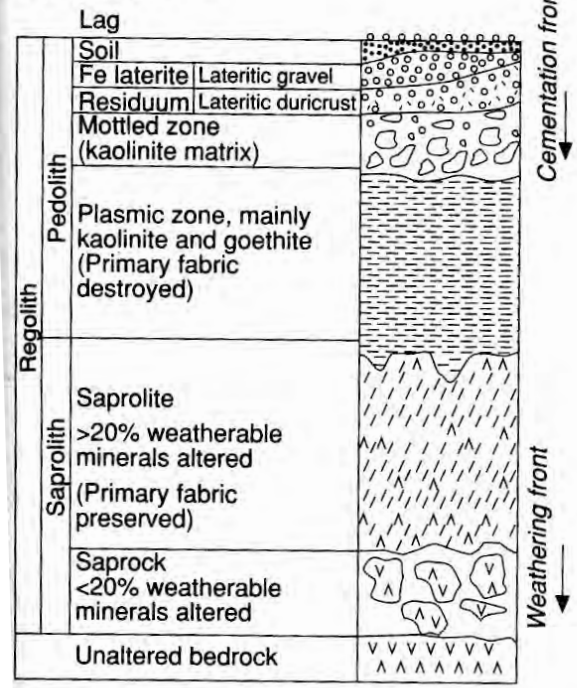

(b) Element mobility in typical lateritic profiles

Host minerals	Leached	Partly retained (in secondary minerals)
Released in the mottled and ferruginous zones		
Aluminosilicates (muscovite, kaolinite) iron oxides; gold	K, Rb, Cs Trace elements; Au	Si, Al (kaolinite)
Released in upper saprolite		
Aluminosilicates (muscovite)	Cs, K, Rb	Si, Al (kaolinite)
Ferromagnesians (chlorite, talc, amphibole)	Mg, Li	Fe, Ni, Co, Cr, Ga, Mn, Ti, V (Fe and Mn oxides)
Smectite clays	Ca, Mg, Na	Si, Al (kaolinite)
Released in the lower saprolite		
Aluminosilicates	Ca, Cs, K, Na, Rb	Si, Al (kaolinite); Ba (barite)
Ferromagnesians (pyroxene, olivine amphiboles, chlorite, biotite)	Ca, Mg	Fe, Ni, Co, Cr, Ga, Mn, Ti, V (Fe and Mn oxides)
Released at weathering front		
Sulfides	As, Au, Cd, Co, Cu, Mo, Ni, Zn, S	As, Cu, Ni, Pb, Sb, Zn, (Fe oxides; sulfates, arsenates, carbonates, alunite-jarosite)
Carbonates	Ca, Mg, Fe, Mn, Sr	

Figure 4.3 (a) A generalized lateritic regolith profile showing the different horizons and the terminology used in their description. (b) Generalized pattern of element mobility in lateritic regoliths (after Butt *et al.*, 2000).

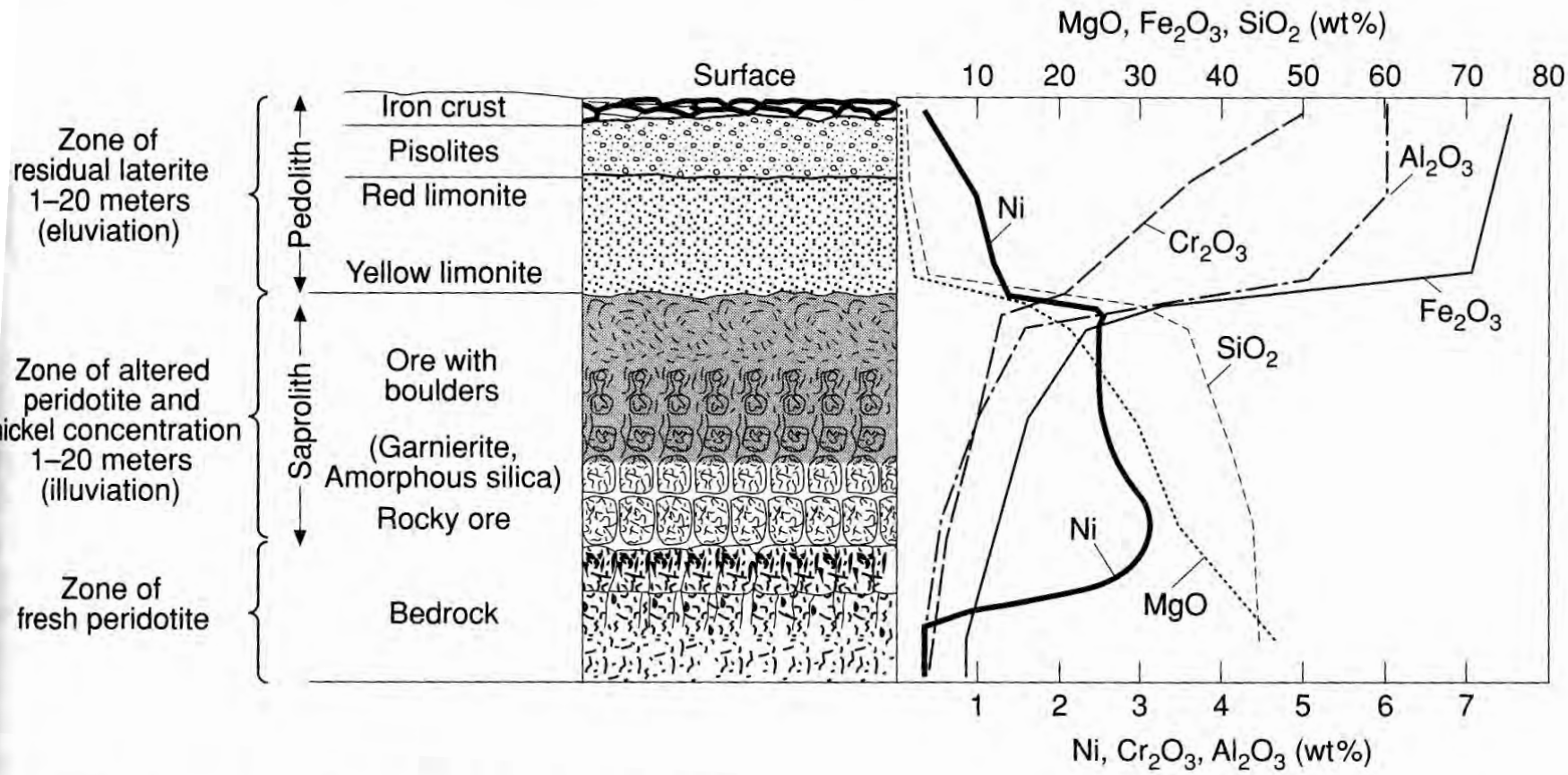

Figure 4.5 Descriptive profile and Ni ore distribution in a lateritic regolith typical of the New Caledonian deposits. The chemical profile clearly distinguishes the ferruginous/aluminous residual zone where Si, Mg, and Ni are leached, from the saprolith where illuviation has resulted in concentration of Ni (after Troly *et al.*, 1979; Guilbert and Park, 1986).

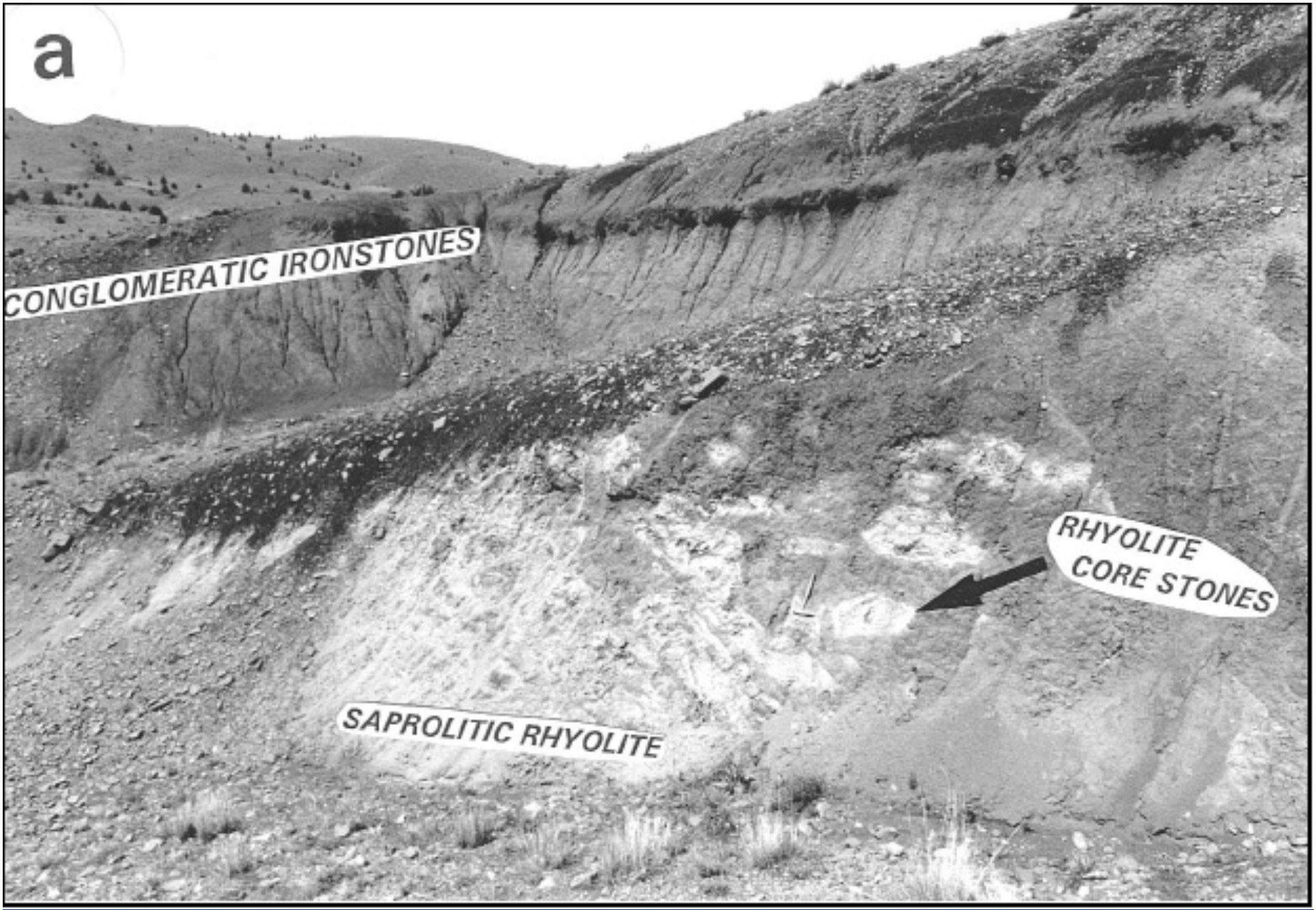

Bestland et al 1996

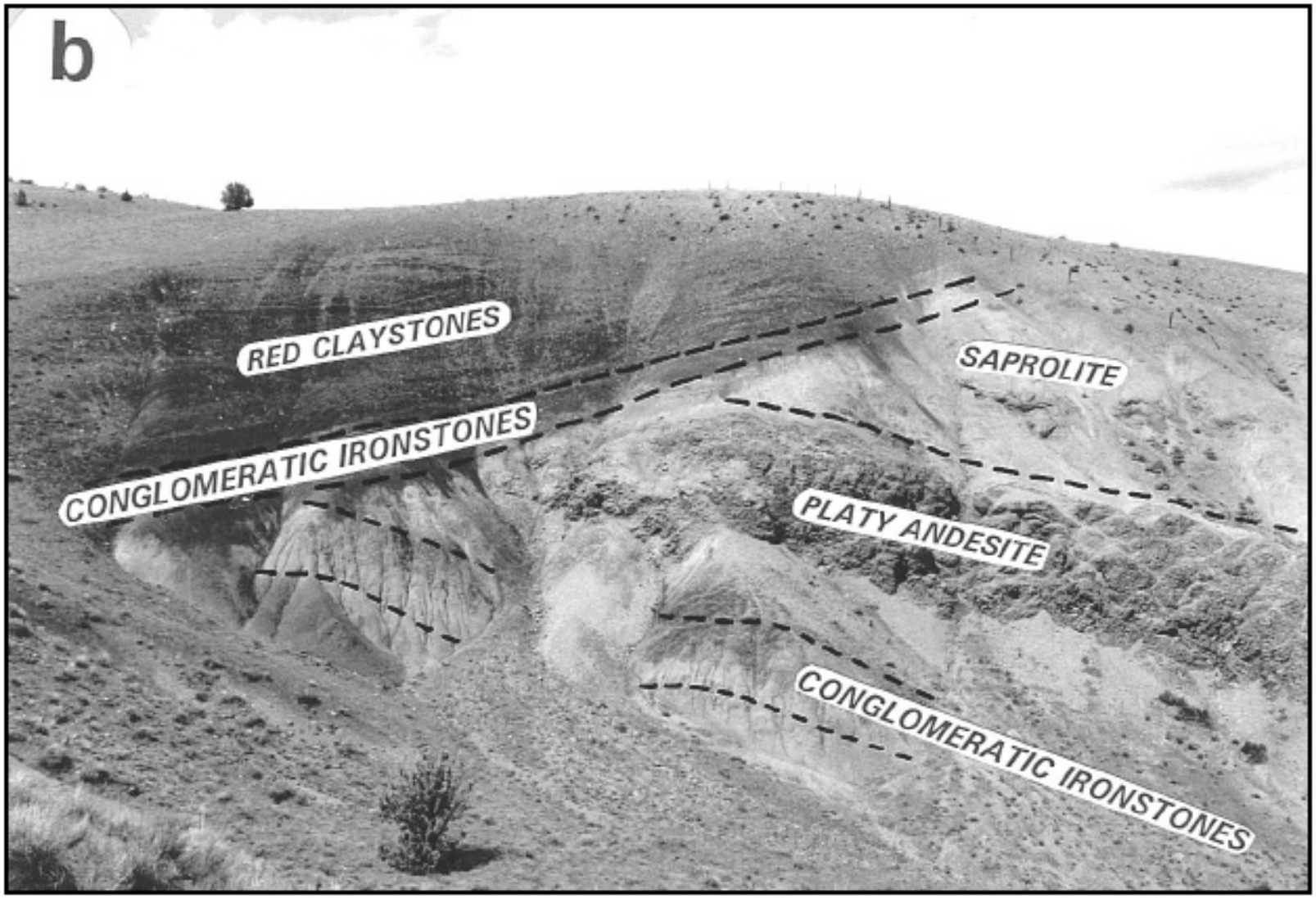

Figure 5. (a) Core-stones of saprolitic rhyolite with overlying conglomeratic ironstone horizons from locality 500 m west of "Brown Grotto" (Fig. 3). (b) Angular discordance between two sequences of conglomeratic ironstones. Lower sequence is associated with the andesite of Bridge Creek Canyon, and the upper sequence, which truncates the lower, is part of the red claystones of "Brown Grotto" associated with the rhyolite of Bear Creek.

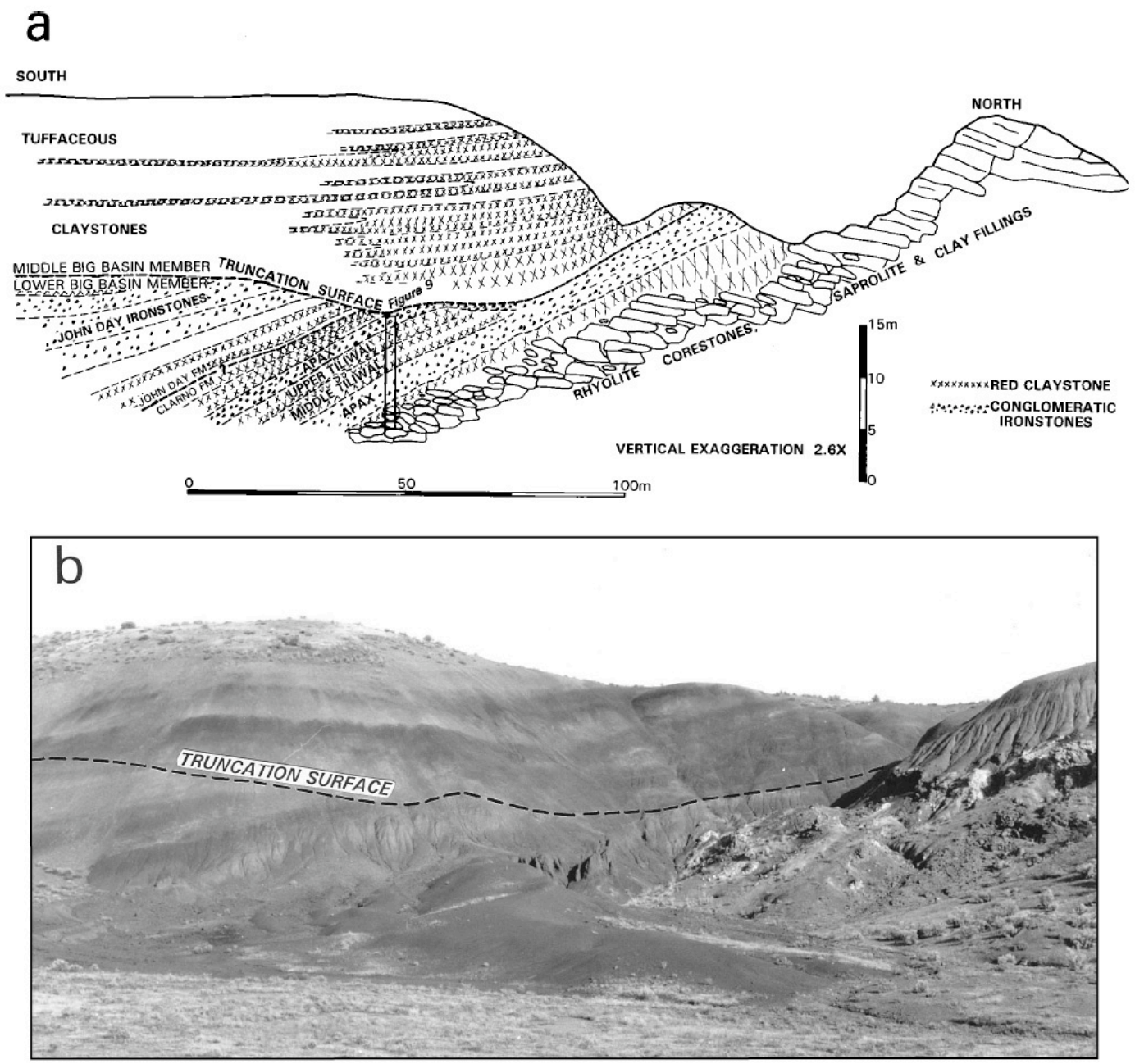

Figure 6. (a) Line drawing of the "Brown Grotto" badlands. (b) Photograph of the "Brown Grotto" badlands viewed from the east.

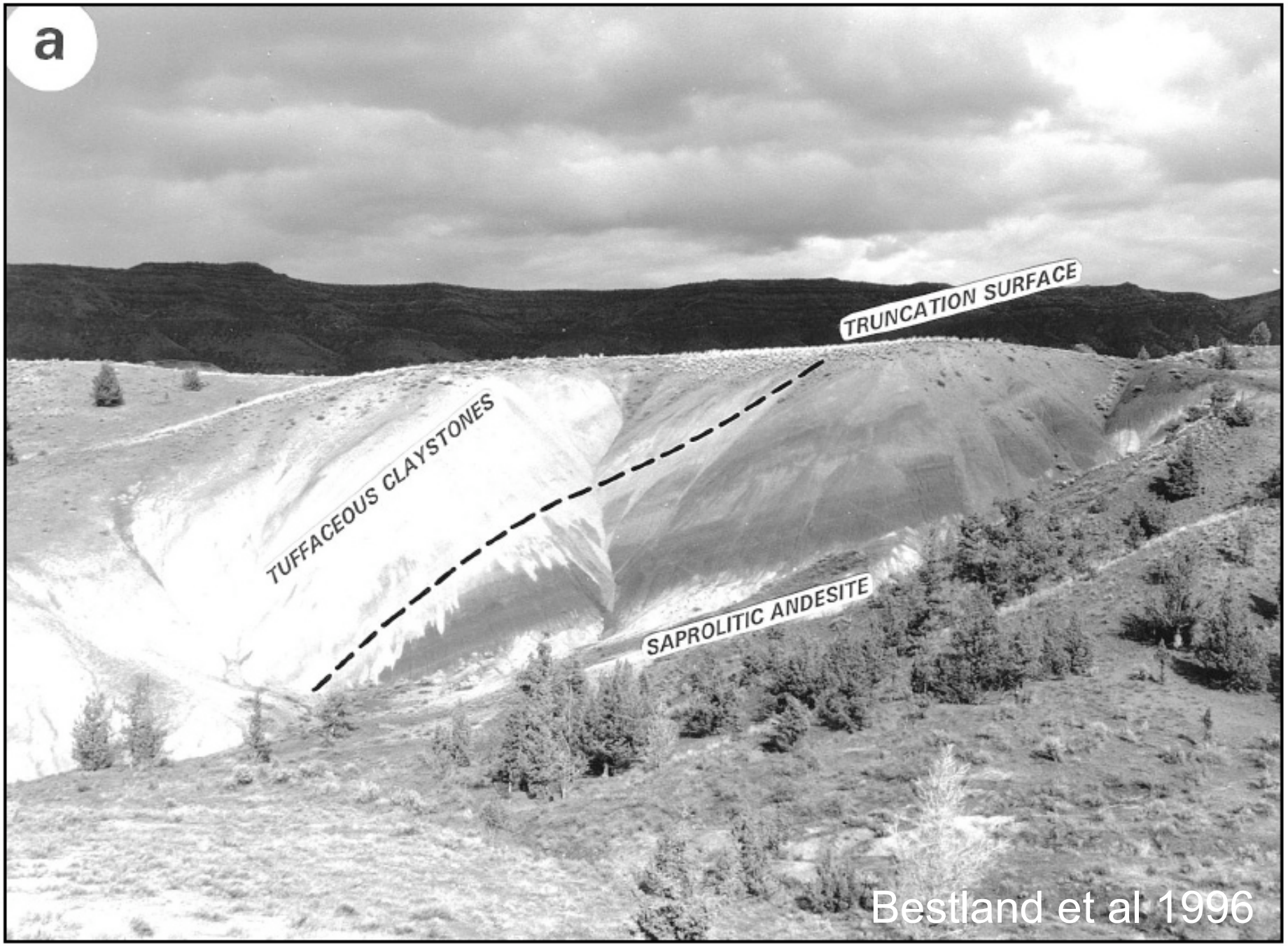
a
TRUNCATION SURFACE
TUFFACEOUS CLAYSTONES
SAPROLITIC ANDESITE
Bestland et al 1996

Figure 8. (a) "Red Ridge" locality viewed from the west. The truncation surface between the lower red claystones and the upper light-colored claystones marks the Eocene-Oligocene boundary. (b) Close-up of "Red Ridge" locality showing gradational contact between the saprolitic andesite breccia and the overlying red claystones.

Bestland et al 1996

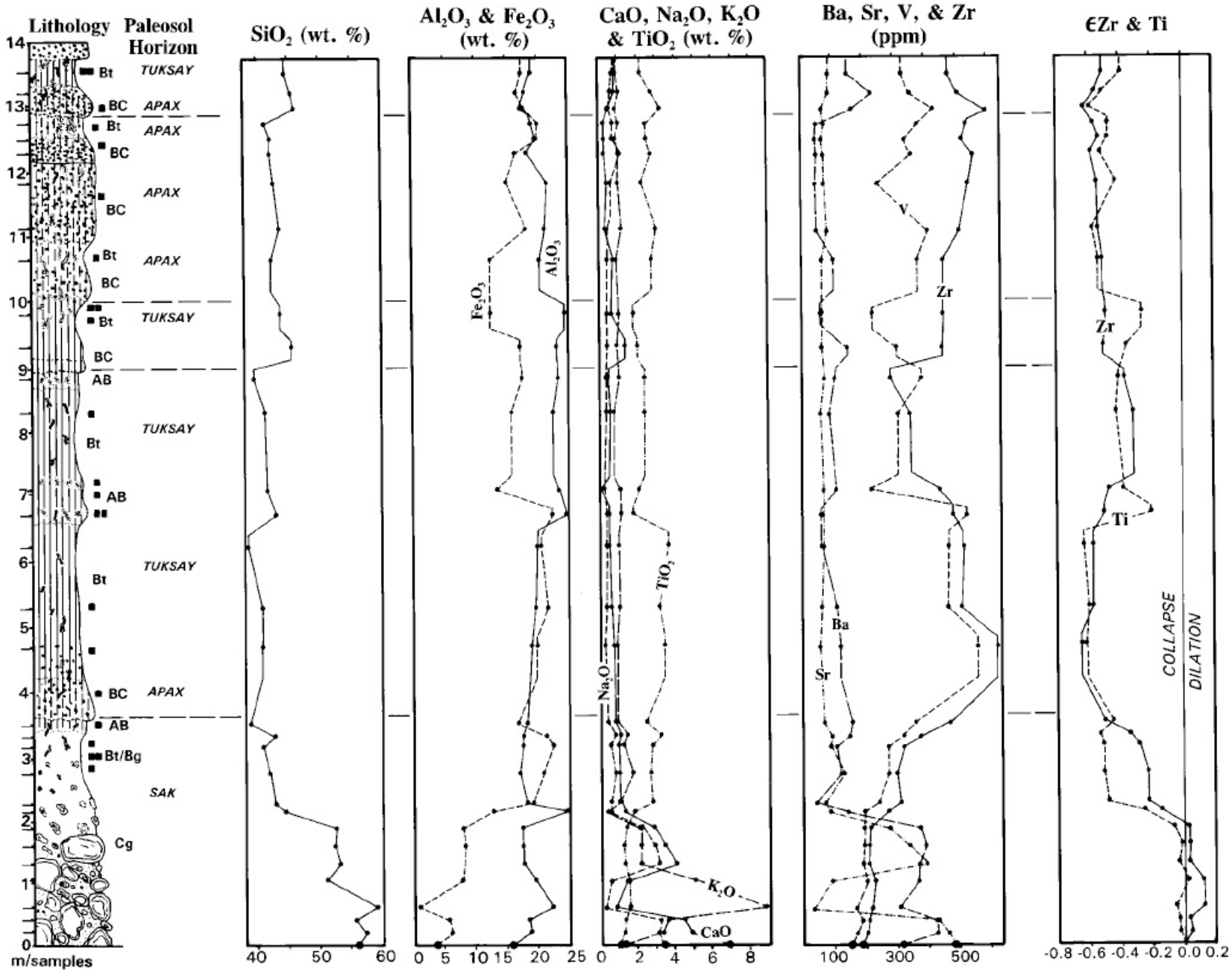

Figure 11. "Red Ridge" stratigraphic section with corresponding bulk-rock (X-ray fluorescence) geochemical depth functions and strain calculated for Ti and Zr, assuming parent material composition of andesite (andesite of Sand Mountain) shown on the bottom axis.

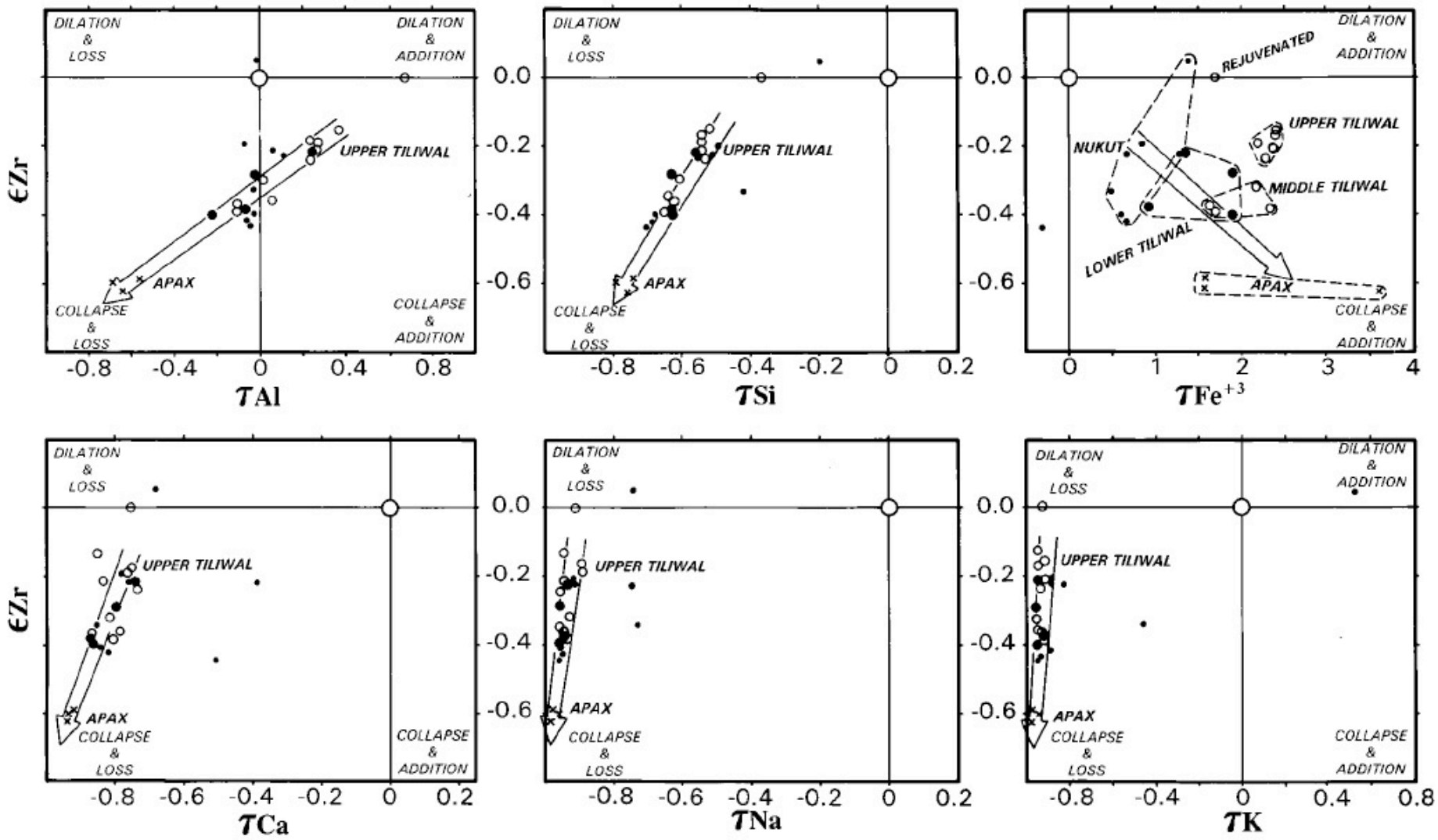

Figure 14. Strain and mass-transport diagrams of paleosol horizons from the "Brown Grotto."

Bestland et al 1996

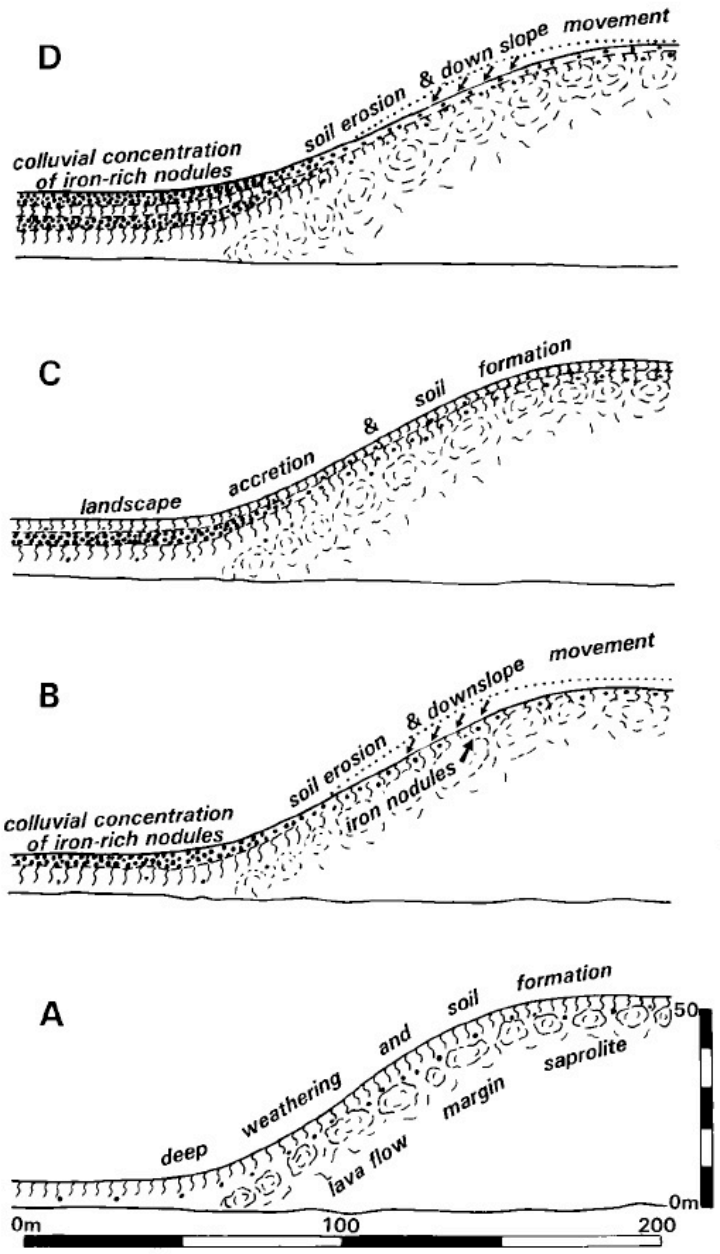

Figure 16. Model for the formation of the "Brown Grotto" detrital laterites (Apax paleosols) and kaolinite-rich, clayey Tiliwal paleosols. The accumulation of iron nodules in toe-slope locations concentrated from erosion of up-slope soil follows detrital laterite model of McFarlane (1976, Fig. 14).

scenario is envisioned in which colluvial pulses of iron-cemented nodules moved downslope as a colluvial lag and were deposited on the toe slopes of hills (lava flows). Upper Clarno Formation colluvium became increasingly weathered and rich in resistate constituents over time. This increase in weathering indicates a lack of soil rejuvenation and probably reflects a paucity of pyroclastic volcanism in the Painted Hills area during the end of volcanic activity in the Clarno arc. Detrital laterites in the lower John Day Formation differ from the Clarno ones in that they contain a few percent pyrogenic crystals. No increase in weathering is observed over time for the John Day laterites, which probably indicates rejuvenation of the landscape by pyroclastic air fall during the early stages of volcanic activity in the Cascade arc and vicinity. The similarity in the textures and compositions of the detrital laterites and associated paleosols indicates that climate remained paratropical and humid during deposition of the lower John Day Formation until a time very close to the Eocene-Oligocene boundary.

Bestland et al 1996

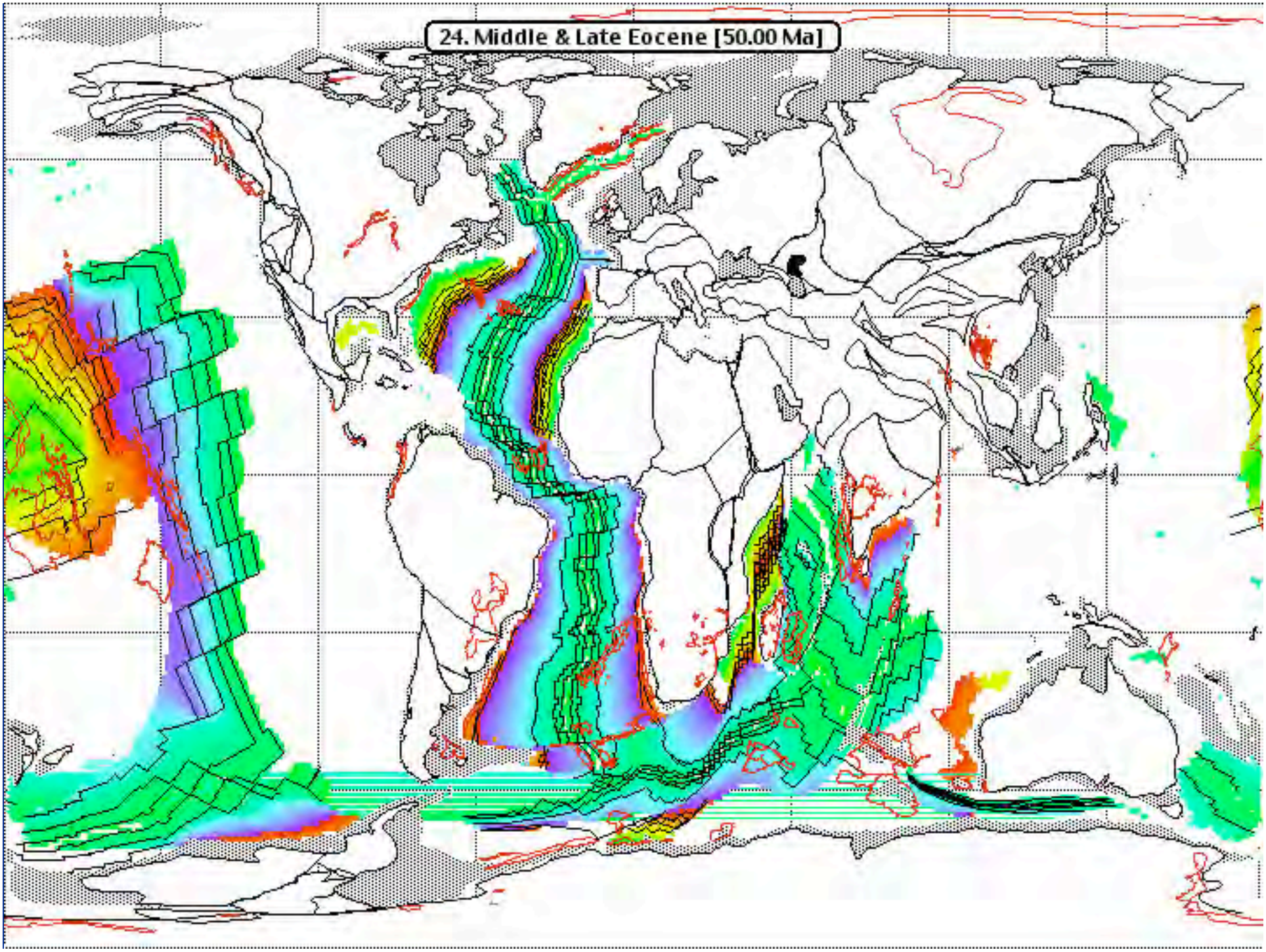
24. Middle & Late Eocene [50.00 Ma]

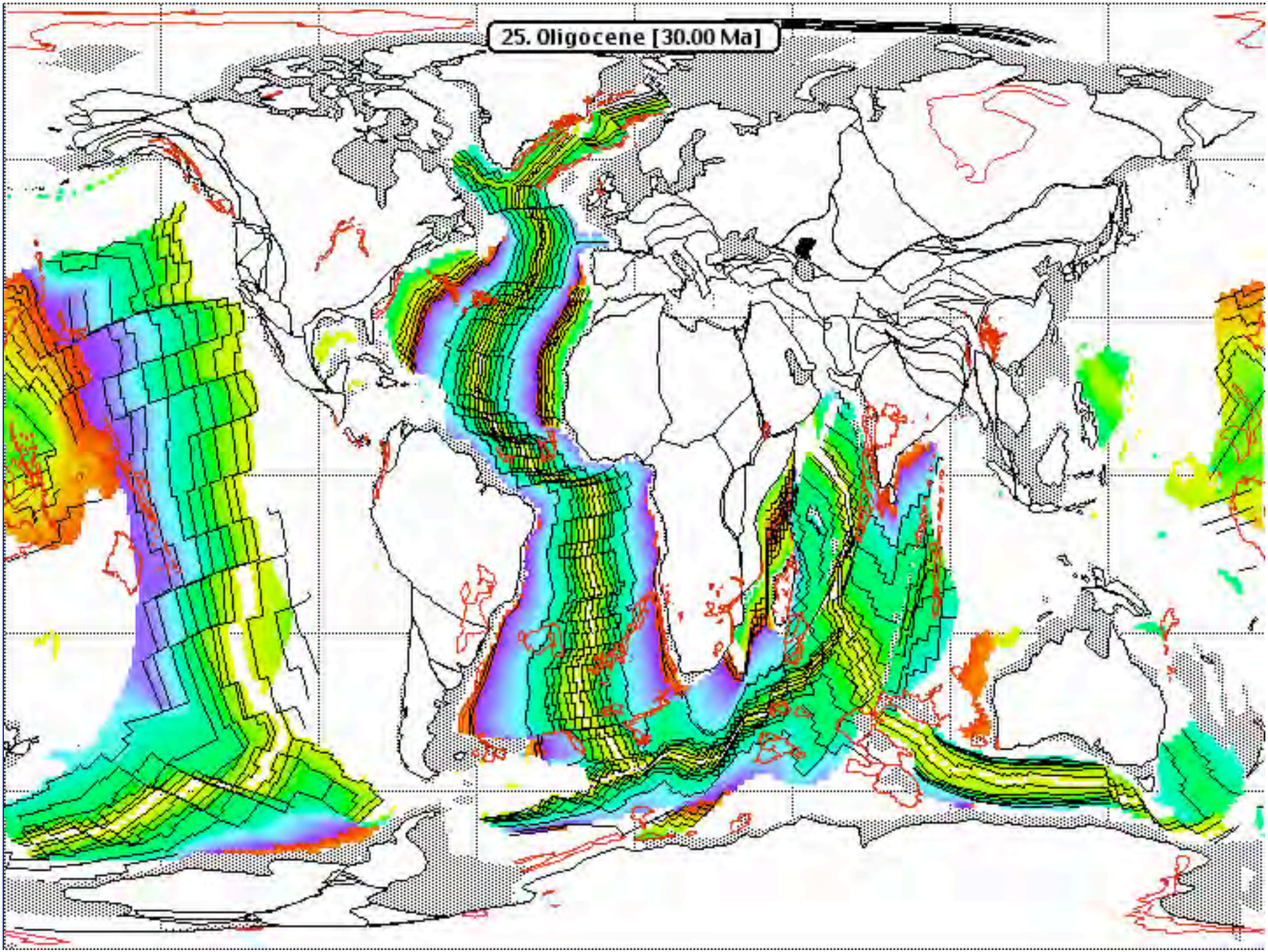
25. Oligocene [30.00 Ma]

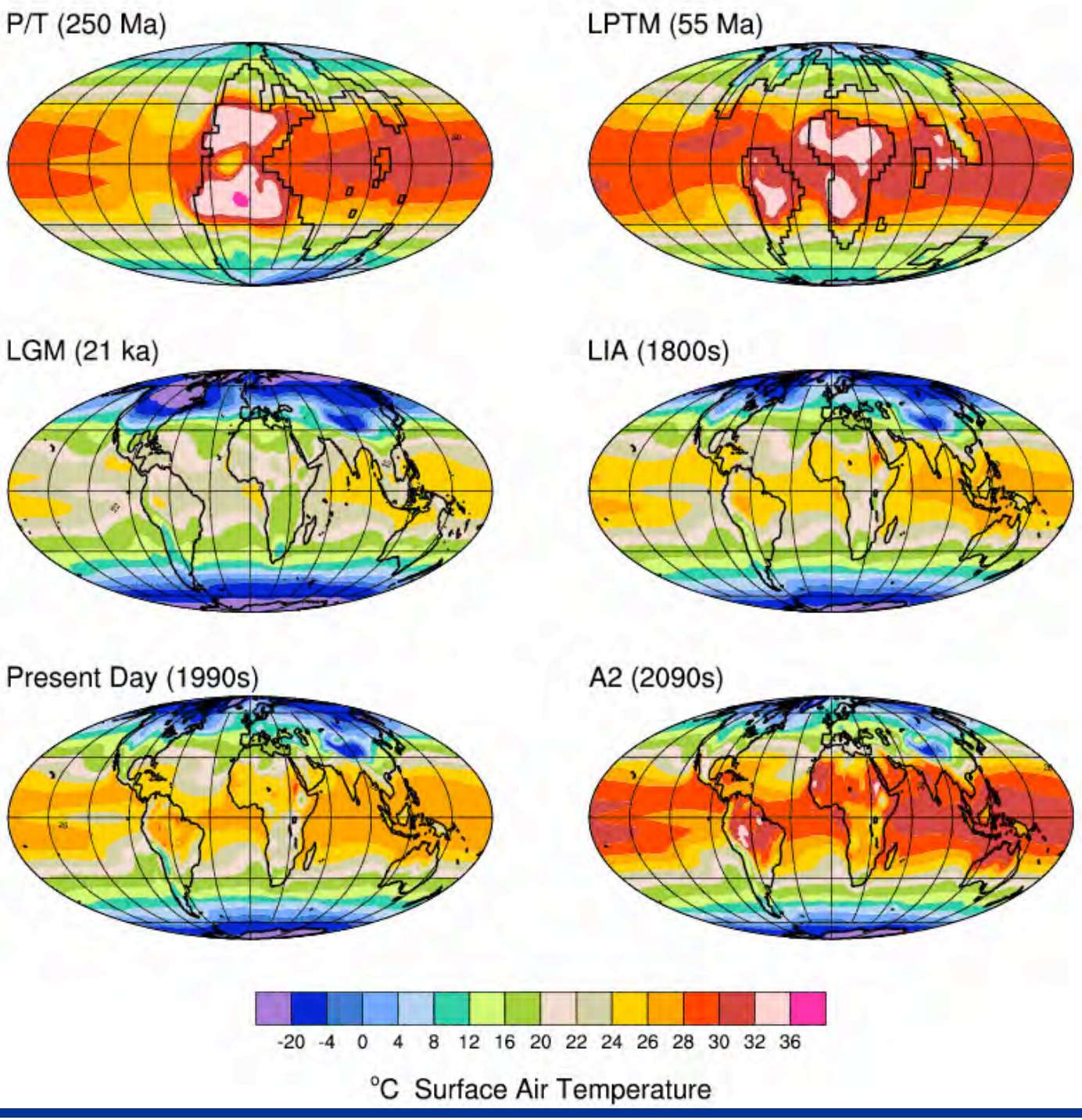

Paleoclimate Models Past, Present, Future

http://www.nesl.ucar.edu/LAR/2007/strategic-priorities/sp1/images/sp1_cgd_1i.jpg